

RIVM Report 680180001/2010

Dynamical version in PDF-format; see changes section

## **Description of the DEPAC module**

Dry deposition modelling with DEPAC\_GC2010

M.C. van Zanten  
F.J. Sauter  
R.J. Wichink Kruit  
J.A. van Jaarsveld, PBL  
W.A.J. van Pul

Contact:  
Margreet van Zanten  
Centrum voor Milieumonitoring  
margreet.van.zanten@rivm.nl

This investigation has been performed by order and for the account of the ministry of Housing, Spatial Planning and the Environment (VROM), within the framework of project M/680180/10/AG Ammonia

© RIVM 2010

Parts of this publication may be reproduced, provided acknowledgement is given to the 'National Institute for Public Health and the Environment', along with the title and year of publication.

## **Changes with respect to the original RIVM Report 680180001**

2012-10-29, Ferd Sauter: In appendix B, a table has been added of parameters that have to be reset, if the number of land use classes is extended.

2013-09-17: vapour pressure deficit (Monteith): corrected erroneous  $T$  in constant term  $a_1$ .

# Abstract

## Description of the DEPAC module

Dry deposition modelling with DEPAC\_GCN2010

The process of dry deposition represents the coming down of air components like ammonia on vegetation and soils. Since dry deposition measurements are difficult and expensive, dry deposition estimates are mainly computed through modelling. New insights have led to an update of the description of the dry deposition process. This report presents a detailed description of the revised software-module DEPAC, which simulates the dry deposition process of ammonia.

Dry deposition influences the concentration of a component in the air and is an important source of components for the receiving surface. Thus it is important to estimate the amount of total nitrogen deposited on nature. When too much nitrogen is deposited, biodiversity is harmed since nitrogen-thrifty vegetation is replaced with more common species like grasses and brambles. Dry deposition of ammonia represents the largest amount of the total nitrogen deposition. Ammonia enters the air predominantly through the process of evaporation from manure in animal stables and when liquid manure is spread over the land.

Earlier versions of the DEPAC module ignored the ammonia concentration in vegetation and soils. The current version assumes that ammonia is present in vegetation, water surfaces and soils. Thus surfaces not only adsorb ammonia but also are able to emit it under certain atmospheric conditions. Further included in the update are an improved description of the light fall in woods and other high vegetation and an improved description of the yearly cycle of the amount of leaf area of plants and trees.

Key words:

dry deposition, ammonia,  $\text{NH}_3$ , compensation point, DEPAC



# Rapport in het kort

## Beschrijving van de DEPAC module

Droge depositie modellering met DEPAC\_GCN2010

Droge depositie is het proces waarbij een stof uit de lucht op de bodem en vegetatie terecht komt. Metingen van het depositieproces zijn omslachtig en duur, daarom wordt de droge depositie met behulp van modellen berekend. Als gevolg van nieuwe inzichten in het droge depositieproces van ammoniak heeft het RIVM de modellering ervan verbeterd. Het rapport beschrijft gedetailleerd de aangepaste softwaremodule (DEPAC) waarmee het droge depositieproces van ammoniak wordt berekend.

Droge depositie beïnvloedt de concentratie van de stof in de lucht en is een belangrijke bron van stoffen voor het ontvangende oppervlak. Zo is het van groot belang inzicht te krijgen in de hoeveelheid droge depositie van stikstof op natuurgebieden. Als teveel stikstof deponert op natuurgebieden, neemt de soortenrijkdom af. Dat komt doordat stikstofminnende planten, zoals grassen en bramen, kwetsbare soorten verdringen. Droge depositie van ammoniak vormt de grootste bijdrage aan de totale stikstofdepositie. Ammoniak komt voornamelijk in de atmosfeer terecht als mest in stallen verdampt of over het land wordt uitgereden.

De vorige modelversie verwaarloosde de ammoniakconcentratie in de vegetatie en de bodem. De huidige versie veronderstelt dat er ammoniak in de vegetatie, wateroppervlakken en de bodem aanwezig is. De vegetatie neemt daarom niet alleen ammoniak op, maar geeft – onder bepaalde atmosferische omstandigheden – ook ammoniak af aan de lucht. Verder is in de software de beschrijving van zonlichtinval in bossen verbeterd, evenals het jaarlijkse verloop van het bladoppervlak van de vegetatie.

Trefwoorden:

droge depositie, ammoniak,  $\text{NH}_3$ , compensatiepunt, DEPAC



# Preface

The deposition module DEPAC (DEPosition of Acidifying Compounds) is available for the calculation of dry deposition fluxes. DEPAC is for instance implemented in the Operational Priority Substance (OPS) model for calculating the large scale deposition maps of the Netherlands (called GDN maps). This technical report describes the entire, updated DEPAC module, version number 3.11. It is mainly aimed at users who want to have a detailed description of all parameterizations in use in DEPAC. This report, however, does not contain an instruction manual.

For those readers who are mainly interested in getting an overview of the updates implemented in DEPAC version 3.11, it would suffice to read Chapter 2. Description of the various exchange pathways of dry deposition can be found in Chapters 3 till 7, while further details of various aspects of the module can be found in the Appendices.

People interested in the effect of the DEPAC update on the GDN maps are referred to Velders et al., 2010.





# Contents

<b>Summary</b>	<b>12</b>
<b>1 Introduction</b>	<b>14</b>
<b>2 Overview of the DEPAC update.</b>	<b>16</b>
<b>3 Dry deposition using a compensation point model</b>	<b>18</b>
<b>4 External leaf surface exchange</b>	<b>22</b>
<b>5 Soil exchange</b>	<b>24</b>
<b>6 Stomatal exchange</b>	<b>26</b>
6.1 Correction for light	27
6.2 Correction for temperature	27
6.3 Correction for vapour pressure deficit	28
6.4 Correction for soil water potential	28
6.5 Correction for phenology	28
<b>7 Exchange in case of snow</b>	<b>30</b>
<b>References</b>	<b>32</b>
<b>Appendix A. Description of DEPAC v3.3</b>	<b>34</b>
<b>Appendix B. Land use and leaf area index</b>	<b>38</b>
<b>Appendix C. Radiation model Weiss and Norman</b>	<b>43</b>
<b>Appendix D. Radiation/leaf model Norman and Zhang</b>	<b>47</b>
<b>Appendix E. Stomatal resistance</b>	<b>51</b>
<b>Appendix F. Compensation points</b>	<b>57</b>
<b>Appendix G. Fluxes and mass balance</b>	<b>65</b>
<b>Appendix H. Implementation issues</b>	<b>69</b>



## Summary

For many years, a difference of roughly 25% existed between the ammonia concentrations as measured by the Dutch Monitoring Network and the ammonia concentrations as modelled by the Operational Priority Substance (OPS) model (Van Jaarsveld, 2004). In Van Pul et al. (2008) the combination of factors leading to this so called 'ammonia gap' are described. Too high dry deposition fluxes of ammonia in OPS were one of them, leading to an underestimation of the concentration of ammonia in the air. In this report the subsequent update of the dry deposition processes is described.

Focus of the update has been on the parameterizations specifically in use for ammonia, although changes have been made that affect other components as well (if the updated version is applied to those components). The major changes are:

1. For ammonia, so called compensation points have been implemented for the stomatal, external leaf surface and soil exchange pathway.
2. The external leaf surface resistance of ammonia has been replaced by the one of Sutton and Fowler (1993), which should be used in combination with the external leaf surface compensation point.
3. The stomatal resistance scheme of Wesely (1989) has been replaced by the more process oriented stomatal resistance scheme of Emberson (2000a, b). This change has an impact on all components.
4. The leaf area index has been taken from Emberson (2000a). This change has an impact on all components.
5. The in-canopy resistance for land use classes *grass* and *other* is set to missing. This change has an impact on all components.
6. Some changes have been made in order to make the former DEPAC versions used for LOTOS-EUROS and OPS consistent. These changes have an impact on NO and SO<sub>2</sub>.



# 1 Introduction

For many years, a systematic difference of roughly 25% existed between the ammonia concentrations as measured by the Dutch Monitoring Network (LML) and the ammonia concentrations as modelled by the Operational Priority Substance (OPS) model (Van Jaarsveld, 2004). In Van Pul et al. (2008) the combination of factors leading to this so called ‘ammonia gap’ are described. Too high dry deposition fluxes of ammonia in OPS were one of them, leading to an underestimation of the concentration of ammonia in the air. As a consequence, the module estimating the dry deposition flux has been revised. During the revision most attention has been paid to an update of the dry deposition of ammonia.

This report describes the entire, updated DEPAC (DEPosition of Acidifying Compounds) module, version number 3.11. This report, however, does not contain an instruction manual of the module, e.g. a detailed list of recommended parameter settings etc. Furthermore, no results of sensitivity tests or validation results are presented. The report contains solely a detailed description of all parameterizations in use in DEPAC. A concise description of an older DEPAC (version 3.3) currently still in use, is given in Appendix A. The original version of DEPAC has been documented in Erisman et al. (1994). DEPAC is implemented in OPS (Van Jaarsveld, 2004), but also in LOTOS-EUROS (Schaap, 2008).

For the calculations of the large scale concentration maps (called GCN-maps) of 2009 (released March 2010) two versions of DEPAC are in use for the various gaseous components. The updated version (version number 3.11) is applied for NH<sub>3</sub> and the older version (version number 3.3) is applied for the other components: HNO<sub>3</sub>, NO, NO<sub>2</sub>, O<sub>3</sub>, SO<sub>2</sub>. The shell around these two DEPAC versions is named DEPAC\_GC2010. Implementation of the new version for the other components besides ammonia, is foreseen after more thorough testing of the update for those components. Revision of the code specific for those components might be necessary.

Due to the update of the DEPAC module, the systematic overestimation of the dry deposition velocity for ammonia above land use class *grass* has been reduced. This has contributed substantially towards the closure of the ammonia gap (Velders et al., 2010). Proper validation of the updated DEPAC module is hampered by the lack of dry deposition measurements. Up till now most deposition measurements are used to construct the deposition parameterization itself and as such cannot be used for validation. The uncertainty in the local dry deposition velocity is estimated to be a factor two. This is an educated guess and further research is a prerequisite to specify the uncertainty more accurately. Both a validation study as well as an uncertainty analysis is planned for the near future.



## 2 Overview of the DEPAC update.

Dry deposition is parameterized using the well-known resistance approach, where the deposition flux is the result of a concentration difference between atmosphere and earth surface and the resistance between them. The current DEPAC versions compute only the so called canopy resistance,  $R_c$ . The aerodynamic resistance for the turbulent layer,  $R_a$ , and the boundary-layer resistance,  $R_b$ , are calculated outside DEPAC.

Focus of the update has been on the parameterizations specifically in use for ammonia, although changes have been made that affect all components (in the case that v.3.11 is applied to those components). The major changes, either in code size or in impact, in v.3.11 compared to v.3.3 are:

1. For ammonia, so called compensation points have been implemented for the stomatal, external leaf surface and soil exchange pathway (Wichink Kruit et al., 2010).
2. The external leaf surface resistance of ammonia has been replaced by the one of Sutton and Fowler (1993), which should be used in combination with the external leaf surface compensation point (Wichink Kruit et al., 2010).
3. The stomatal resistance scheme of Wesely (1989) has been replaced by the more process oriented stomatal resistance scheme of Emberson (2000a, b). This change has an impact on all components.
4. The leaf area index has been taken from Emberson (2000a). This change has an impact on all components.
5. The in-canopy resistance for land use classes *grass* and *other* is set to missing. This change has an impact on all components.
6. Some changes have been made in order to make the former DEPAC versions used for LOTOS-EUROS and OPS consistent. These changes have an impact on NO and SO<sub>2</sub>.

The above changes will be described in more detail below. Full details can be found in the rest of the report.

*1. Compensation points.* Up till now, only deposition fluxes were calculated in DEPAC and no emission fluxes were allowed. In the current version, the flux is allowed to be bidirectional by including compensation points in the stomatal, external leaf surface and the soil exchange pathway (see Figure 1 for a schematic picture). Compensation points are in use for all land use classes. (Chapter 3).

Both the stomatal and the external leaf surface compensation point depend on temperature and ammonia concentration in the air. However, the stomatal compensation point represents the ammonia present in the vegetation and thus is tied to a fairly long timescale (e.g. the local yearly mean). Since ammonium concentrations in water layers present on leaves have a short memory, the external leaf compensation point is linked to the actual ammonia concentration in the air. Both compensation point parameterizations have been derived based on three years of measurements of ammonia fluxes over a grassland canopy (Wichink Kruit et al., 2010). (Chapter 6 and chapter 4).

For the soil compensation point not enough information is known to implement a parameterization, so this variable is currently set to zero. Only for land use class *water* a simple water compensation point parameterization with a dependency on water temperature is derived, based on five years of measurements at several locations in fresh water bodies and the North Sea. This parameterization is in first instance valid for Dutch locations only. (Chapter 5).



2. *External leaf surface resistance.* The external leaf surface resistance for ammonia is based on Sutton and Fowler (1993) and is dependent on ambient relative humidity only. This parameterization is representative for clean air; the influence of pollution is accounted for in the external leaf surface compensation point value. The Sutton and Fowler parameterization should always be used in combination with a compensation point, since neglecting this compensation point would lead to an overestimation of ammonia deposition through the external leaf exchange pathway. (Chapter 4).

3. *Stomatal resistance.* The stomatal resistance scheme of Emberson (2000a,b) has been implemented; this scheme is also in use in the European Modelling and Evaluation Programme (EMEP) model. In this scheme, several factors are used to scale a minimal resistance value. One factor takes into account the availability of light; in this factor a difference is made between direct and diffuse sunlight on sunlit and shaded leaves. Other environmental factors accounted for are temperature and water vapour deficit. The phenological factor of the Emberson scheme is not implemented, since this factor is negligible for the land use classes used in DEPAC. The effect of a deficit of soil moisture is not implemented either. (Chapter 6).

4. *Leaf area index.* The monthly changing Leaf Area Index (LAI) values have been replaced by ones with a dependency on the day of year to ensure a better representation of the growing season (Emberson, 2000a). A latitude dependent effect on the length of the growing season is now also included. The LAI is used in the upscaling of the leaf stomatal resistance to a stomatal resistance valid for the whole canopy. A Surface Area Index (SAI) has been introduced for the upscaling of the external leaf resistance from leaf to canopy scale. SAI is commonly larger than LAI due to the presence of branches and stems. (Appendix B).

5. *In-canopy resistance.* The in-canopy resistance for land use class *grass* (and *other* since this class is modelled identically to *grass*) is set to missing instead of zero. This shuts off the soil exchange path completely. (Chapter 5).

6. *Changes for consistency.* Before this DEPAC update, a few differences existed between the OPS DEPAC version and the LOTOS-EUROS version with regard to SO<sub>2</sub> and NO. In version 3.11 these differences are straightened, in which Erisman et al. (1994) has been guiding. See Appendix H.

### 3 Dry deposition using a compensation point model

In the dry deposition module DEPAC, dry deposition is parameterized using the well-known resistance approach, where the deposition flux is the result of a concentration difference between atmosphere and earth surface and the resistance between them. Several pathways exist for the deposition flux, each with its own resistance and concentration. In DEPAC three pathways are taken into account:

- through the stomata (subscript *s*);
- through the external leaf surface (water layer or cuticular waxes, subscript *w*); and
- through the soil (subscript *soil*).

The concentration in the stomata, at the external leaf surface or at the soil surface is for historic reasons called a *compensation point*.

A schematic representation of concentrations  $\chi$ , resistances  $R$  and fluxes  $F$  is given in Figure 1.

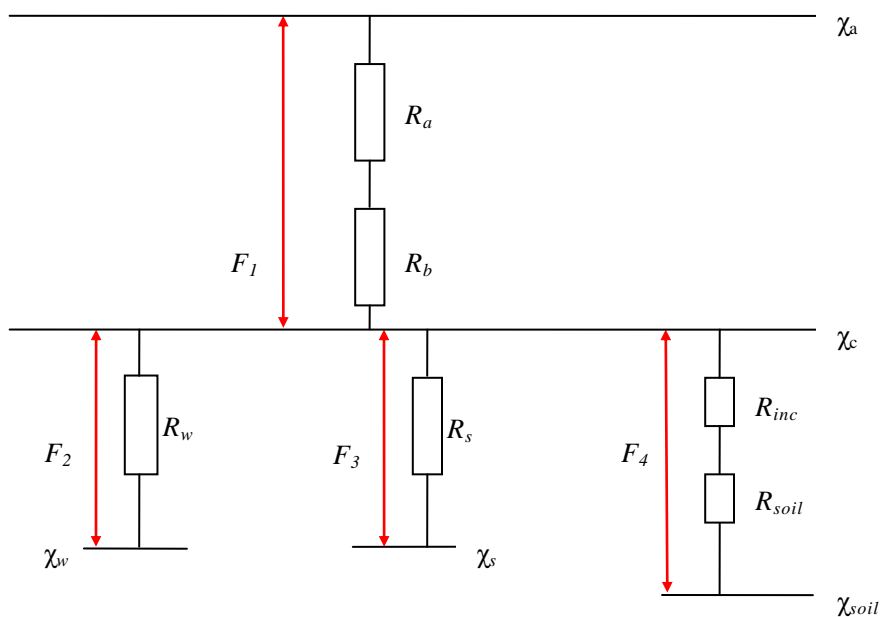


Figure 1. Schematic representation of resistance approach with compensation points.

name of parameter	unit	name in DEPAC	explanation
$\chi_a$	$\mu\text{g}/\text{m}^3$	<i>catm</i>	concentration in air
$\chi_c$	$\mu\text{g}/\text{m}^3$		concentration at canopy top
$\chi_w$	$\mu\text{g}/\text{m}^3$	<i>cw</i>	concentration at external leaf surface
$\chi_{soil}$	$\mu\text{g}/\text{m}^3$	<i>csoil</i>	concentration at soil surface
$\chi_s$	$\mu\text{g}/\text{m}^3$	<i>cstom</i>	concentration in stomata
$R_a$	s/m	<i>ra</i>	aerodynamic resistance
$R_b$	s/m	<i>rb</i>	quasi-laminar layer resistance
$R_w$	s/m	<i>rw</i>	external leaf surface or water layer resistance, <i>also called</i> cuticular resistance
$R_s$	s/m	<i>rstom</i>	stomatal resistance
$R_{inc}$	s/m	<i>rinc</i>	in canopy resistance
$R_{soil}$	s/m	<i>rsoil</i>	soil resistance
$R_{soil,eff}$	s/m	<i>rsoil_eff</i>	effective soil resistance = $R_{inc} + R_{soil}$
$R_c$	s/m	<i>rc_tot</i>	canopy resistance

In the text below, we distinguish between upper case and lower case characters:

- $r$ : leaf resistance;
- $R$ : canopy averaged resistance;
- $g$ : leaf conductance =  $1/r$ ;
- $G$ : canopy averaged conductance  $G = 1/R$ .

For the external leaf conductance,  $G = SAI g$ , with  $SAI$  = surface area index (i.e. the area of leaves, branches and stems per unit area of ground surface).

For the stomatal conductance,  $G = LAI g$ , with  $LAI$  = leaf area index (i.e. the area of leaves per unit area of ground surface).

More information on LAI and SAI can be found in Appendix B.

The fluxes  $F$  over the different pathways in Figure 1 are:

$$F_1 = -\frac{(\chi_a - \chi_c)}{R_a + R_b}, F_2 = -\frac{(\chi_c - \chi_w)}{R_w}, F_3 = -\frac{(\chi_c - \chi_{soil})}{R_{soil,eff}}, F_4 = -\frac{(\chi_c - \chi_s)}{R_s}. \quad (1)$$

$$\text{We define the canopy resistance } R_c = \left( \frac{1}{R_w} + \frac{1}{R_{soil,eff}} + \frac{1}{R_s} \right)^{-1}, \quad (2)$$

$$\text{the exchange velocity } V_e = \frac{1}{R_a + R_b + R_c} \quad (3)$$

$$\text{and the total compensation point } \chi_{tot} = \left[ \frac{R_c}{R_w} \chi_w + \frac{R_c}{R_{soil,eff}} \chi_{soil} + \frac{R_c}{R_s} \chi_s \right]. \quad (4)$$

In Appendix G., we derive the following expression for the flux  $F_1$ :

$$F_1 = -V_e(\chi_a - \chi_{tot}). \quad (5)$$

The mass balance in a layer with height  $H$  is:

$$H \frac{\partial \chi_a}{\partial t} = F_1 = -V_e \cdot (\chi_a - \chi_{tot}). \quad (6)$$

If we assume a constant value of  $\chi_{tot}$  (large reservoir) on a time interval  $[t, t + \Delta t]$ , we get as solution:

$$\chi_a(t + \Delta t) = \chi_{tot} + (\chi_a(t) - \chi_{tot}) \cdot \exp\left(-\frac{V_e}{H} \cdot \Delta t\right). \quad (7)$$

An alternative method (Asman, 1994), that puts the compensation point into an effective resistance, is presented in Appendix G.

In the following sections, we will describe the parameterizations of the different resistances that contribute to the canopy resistance  $R_c$  for dry deposition of  $\text{NH}_3$ . Parameterizations of  $R_a$  and  $R_b$  can be found in Van Jaarsveld (2004).

Resistance parameterizations are different for different land use types. In DEPAC the following land use types are used:

- 1 = grass
- 2 = arable land
- 3 = permanent crops
- 4 = coniferous forest
- 5 = deciduous forest
- 6 = water
- 7 = urban
- 8 = other
- 9 = desert

In the text we will use 'forest' for both coniferous and deciduous forest. For more information on land use classes, see Appendix B.



## 4 External leaf surface exchange

In DEPAC, we use the following parameterization for the canopy averaged external leaf surface resistance:

$$R_w = \frac{SAI_{Haarweg}}{SAI} \alpha \cdot \exp\left(\frac{100 - RH}{\beta}\right), \quad (8)$$

with RH the relative humidity in %,  $\alpha = 2$  s/m,  $\beta = 12$ ,  $SAI$  = surface area index (i.e. the area of leaves, branches and stems per unit area of ground surface) and  $SAI_{Haarweg}$  = surface area index at the Haarweg measuring site (estimated to be 3.5).

The parameterization  $\alpha \cdot \exp\left(\frac{100 - RH}{\beta}\right)$ ,

represents the minimum external leaf surface resistance,  $R_{w,min}$  (Sutton and Fowler, 1993) that only accounts for the relative humidity response and is valid for clean conditions (this assumption is supported by the findings of Milford et al., 2001b). The higher  $R_w$  values at 100% relative humidity found in literature (Nemitz et al., 2001) reflect different air pollution climates, as well as potential variation in  $NH_3$  supply from the canopy itself, which will be accounted for in  $\chi_w$ .

The scaling factor  $\frac{SAI_{Haarweg}}{SAI}$ ,

takes into account that for a different vegetation type, the surface area index of the vegetation may be different from that of the measuring site, for which the parameterization of  $\chi_w$  was derived.

At the external leaf surface water interface, the gaseous  $NH_3$  concentration,  $\chi_w$ , may be considered as being in equilibrium with the dissolved  $NH_4^+$  concentration. The theoretical relationship between the gaseous ammonia concentration, leaf surface temperature ( $T_s$ ), ammonium concentration and pH, can be derived from the temperature response of the Henry equilibrium for ammonia,  $NH_3(g) \leftrightarrow NH_3(aq)$ , and the ammonium-ammonia dissociation equilibrium,  $NH_3(aq) + H^+(aq) \leftrightarrow NH_4^+(aq)$ . The theoretical atmospheric  $NH_3$  concentration at the leaf surface water interface,  $\chi_w$ , can be calculated analogous to the stomatal compensation point (following the formulation of Nemitz et al., 2001, and Wichink Kruit et al., 2007):

$$\chi_w = \frac{2.75 \cdot 10^{15}}{T_s + 273.15} \exp\left(\frac{-1.04 \cdot 10^4}{T_s + 273.15}\right) \cdot \Gamma_w \quad (9)$$

where  $\chi_w$  is the gaseous  $NH_3$  concentration at the external leaf surface ( $\mu g m^{-3}$ ),  $T_s$  is the leaf surface temperature ( $^{\circ}C$ ) and  $\Gamma_w$  is the dimensionless molar ratio between the  $NH_4^+$  and  $H^+$  concentrations in the external leaf surface water.

An empirical relation for  $\Gamma_w$  is derived for grassland by Wichink Kruit et al. (2010):

$$\Gamma_w = 1.84 \cdot 10^3 \cdot \chi_{a,4m} \cdot \exp(-0.11 \cdot T_s) - 850 \quad (10)$$

where  $\chi_{a,4m}$  is the actual atmospheric ammonia concentration at 4 m height in  $\mu g m^{-3}$  and  $T_s$  is the leaf surface temperature in  $^{\circ}C$ .

The functional behaviour of  $\chi_w$  and  $\Gamma_w$  is shown in Appendix F. As can be seen from this appendix, the external leaf compensation point is always smaller than the atmospheric concentration and thus emissions from plant to atmosphere will not take place. Models that do not have the actual atmospheric concentration available may use a long-term averaged concentration. In this case, emission might occur in certain circumstances.

Here, we assume that the parameterization for  $\Gamma_w$  is also valid for other vegetation types, as it is not supposed to be a plant property. Or formulated alternatively, we expect concentration and temperature dependencies to be more important than the dependency on vegetation type.

In freezing conditions  $r_w$  is set to 200 s/m.

## 5 Soil exchange

The soil resistance (s/m) is given as follows (Erisman et al 1994, note that here 0 is interpreted as 'negligible' and the corresponding resistance is set to 10 s/m):

$$\begin{aligned}
 \text{Frozen soil} & : R_{soil} = 1000 \text{ s m}^{-1}. \\
 \text{non-frozen soil, dry} & : R_{soil} = 10 \text{ s m}^{-1}, \text{ water.} \\
 & R_{soil} = 100 \text{ s m}^{-1}, \text{ all other DEPAC land use classes.} \\
 \text{non-frozen soil, wet} & : R_{soil} = 10 \text{ s m}^{-1}.
 \end{aligned} \tag{11}$$

The in-canopy resistance is parameterized as (Van Pul and Jacobs, 1994):

$$\begin{aligned}
 R_{inc} &= \frac{b \cdot h \cdot SAI}{u^*}, & u^* > 0, \text{ arable land, permanent crops, forest.} \\
 R_{inc} &= 1000 \text{ s m}^{-1}, & u^* \leq 0, \text{ arable land, permanent crops, forest.} \\
 R_{inc} &= 0 \text{ s m}^{-1}, & \text{water, urban, desert.} \\
 R_{inc} &= \infty \text{ s m}^{-1}, & \text{grass, other.}
 \end{aligned} \tag{12}$$

with  $b$  an empirical constant ( $14 \text{ m}^{-1}$ ),  $h$  vegetation height (m),  $SAI$  surface area index (-) and  $u^*$  the friction velocity (m/s).

The resistance used for the soil pathway is the effective soil resistance:

$$R_{soil,eff} = R_{inc} + R_{soil}. \tag{13}$$

A soil compensation point  $\chi_{soil}$  is added, analogous to the stomatal compensation point. However, since it is unknown what the best value or best parameterization of  $\chi_{soil}$  should be, its value is currently set to zero. Only for land use class water, a parameterization for  $\chi_{soil}$  (named  $\chi_{water}$  in the text below for clarity) has been added, similar as for  $\chi_w$ :

$$\chi_{water} = \frac{2.75 \cdot 10^{15}}{T_{water} + 273.15} \exp\left(\frac{-1.04 \cdot 10^4}{T_{water} + 273.15}\right) \cdot \Gamma_{water} \tag{14}$$

The necessary  $\Gamma_{water}$  and temperature value are based on five recent years of data from the Waterbase data of Rijkswaterstaat. Based on  $\text{NH}_4^+$  and pH data of seventy stations a representative value for  $\Gamma_{water}$  was derived:

$$\Gamma_{water} = 430. \tag{15}$$

This value is representative for the large water bodies in the Netherlands and the coastal waters, but overestimates  $\chi_{water}$  further away at sea and underestimates  $\chi_{water}$  in polluted rivers and lakes. At 25 of these 70 sites temperature has been measured as well. Based on this data, the following representative yearly cycle of water temperature has been derived:

$$T_{water} = 13.05 + 8.3 \sin(DOY - 113.5) \text{ } ^\circ\text{C} \tag{16}$$

with  $DOY$  = day of year. More detail about the derivation of the parameterization and figures of measurements and parameterized values of  $\chi_{water}$  at several sites are given in Appendix F.





## 6 Stomatal exchange

In the parameterization of the stomatal resistance we follow Emberson (2000a,b). The parameterization shown here is formulated in terms of conductance  $G = 1/R$ . With a lower case  $g$  we denote leaf conductance, upper case  $G$  is used for a canopy averaged conductance.

Emberson uses a maximal stomatal conductance (for certain optimal conditions) that is reduced by different correction factors (between 0 and 1):

$$G_s = G_s^{\max} \cdot f_{phen} \cdot f_{vpd} \cdot f_T \cdot f_{PAR} , \quad (17)$$

with

$G_s$  : canopy averaged stomatal conductance (m/s);

$G_s^{\max}$  : canopy averaged stomatal conductance for optimal conditions (m/s);

$f_{phen}$  : correction factor for phenology (-);

$f_{vpd}$  : correction factor for vapour pressure deficit (-);

$f_T$  : correction factor for temperature (-);

$f_{PAR}$  : correction factor for photoactive radiation (-).

Emberson provides values for the maximal leaf conductance  $g_{s,ref}^{\max}$  for a reference gas (ozone), which has to be multiplied by the leaf area index LAI to obtain a canopy conductance:

$$G_{s,ref}^{\max} = LAI \cdot g_{s,ref}^{\max} . \quad (18)$$

More information on the leaf area index can be found in Appendix B.

In order to obtain the maximal stomatal conductance for another gas than the reference, we multiply with the ratio of the diffusion coefficients:

$$G_s^{\max} = \frac{D}{D_{ref}} G_{s,ref}^{\max} , \quad (19)$$

$D$  : diffusion coefficient of gas (m<sup>2</sup>/s);

$D_{ref}$  : diffusion coefficient of reference gas (m<sup>2</sup>/s).

## 6.1 Correction for light

The correction factor  $f_{PAR}$  for the influence of the sun's radiation on the stomatal resistance is a weighted average of the corrections for sunlit and shaded leaves:

$$f_{PAR,sun} = [1 - \exp(-\alpha PAR_{sun})], \quad f_{PAR,shade} = [1 - \exp(-\alpha PAR_{shade})] \quad (20)$$

$$f_{PAR} = \frac{LAI_{sun}}{LAI} f_{PAR,sun} + \frac{LAI_{shade}}{LAI} f_{PAR,shade}, \quad f_{PAR} = \max(f_{PAR}, f_{min}) \quad (21)$$

with

$PAR$  : photoactive radiation ( $W/m^2$ );

$LAI$  : leaf area index ( $m^2$  leaf /  $m^2$  surface);

$\alpha$  : vegetation-specific parameter in light correction factor ( $[W/m^2]^{-1}$ );

$f_{min}$  : minimal correction factor (-);

$sun$  : sunlit leaves;

$shade$  : shaded leaves.

The parameterization of PAR and LAI for sunlit and shaded leaves is described in Appendices C and D.

## 6.2 Correction for temperature

The correction factor for temperature  $f_T$  is taken from Jarvis, 1976. Note that the publication of Jarvis contains an error in the definition of  $b_T$ ; the correct form is listed below (see also Baldocchi et al., 1987, p. 97). It is a bell-shaped curve, which indicates that stomata are closed due to low temperatures and to very high temperatures:

$$f_T = \left( \frac{T - T_{min}}{T_{opt} - T_{min}} \right) \left( \frac{T_{max} - T}{T_{max} - T_{opt}} \right)^{b_T}, \quad b_T = \left( \frac{T_{max} - T_{opt}}{T_{opt} - T_{min}} \right), \quad f_T = \max(f_T, f_{min}), \quad (22)$$

$T$  : temperature ( $^{\circ}C$ );

$T_{min}$  : minimal temperature for open stomata ( $^{\circ}C$ );

$T_{max}$  : maximal temperature for open stomata ( $^{\circ}C$ );

$b_T$  : factor (-).

$T_{min}$  and  $T_{max}$  are vegetation (and thus land use class) dependent parameters.

### 6.3 Correction for vapour pressure deficit

The vapour pressure deficit is parameterized following Monteith (1973):

$$P_{sat} = a_1 + a_2T + a_3T^2 + a_4T^3 + a_5T^4 + a_6T^5, \quad vpd = P_{sat} \cdot \left(1 - \frac{RH}{100}\right), \quad (23)$$

$P_{sat}$  : saturation vapour pressure (kPa) ;

$T$  : temperature (°C) ;

$a_i$  : coefficient (kPa/°C<sup>(i-1)</sup>),  $a_1 = 6.113718 \cdot 10^{-1}$ ,  $a_2 = 4.43839 \cdot 10^{-2}$ ,  $a_3 = 1.39817 \cdot 10^{-3}$ ,  
 $a_4 = 2.9295 \cdot 10^{-5}$ ,  $a_5 = 2.16 \cdot 10^{-7}$ ,  $a_6 = 3.0 \cdot 10^{-9}$ ;

$RH$  : relative humidity (%);

$vpd$  : vapour pressure deficit (kPa).

The correction factor for vapour pressure deficit is

$$f_{vpd} = (1 - f_{\min}) \left( \frac{vpd_{\min} - vpd}{vpd_{\min} - vpd_{\max}} \right) + f_{\min}, \quad f_{vpd} = \max(\min(f_{vpd}, 1), f_{\min}), \quad (24)$$

with

$vpd_{\min}$  : vapour pressure deficit with minimal conductance (kPa)  $\rightarrow f_{vpd} = f_{\min}$ ;

$vpd_{\max}$  : vapour pressure deficit with maximal conductance (kPa)  $\rightarrow f_{vpd} = 1$ .

### 6.4 Correction for soil water potential

No correction for soil water potential is applied;  $f_{swp} = 1$ . We expect that in North-Western Europe, this factor will be of limited influence; in Southern European countries it may be important, but there is not very much information available to compute this correction factor, see Emberson (2000a).

### 6.5 Correction for phenology

The influence of phenology on stomatal conductance is ignored for now in DEPAC v3.11, since the influence of the functions proposed by Emberson for the land use classes in use in DEPAC is negligible (see appendix B.). When other classes are used (e.g. *Mediterranean broadleaf*),  $f_{phen}$  might be too important to ignore.

The following table lists the parameters involved in the Emberson parameterization. Values in gray-shaded cells are not used in DEPAC, they are included only for comparison with Simpson (2008).

**Table 1. parameters for stomatal conductance from Simpson (2008); -999 in case there is no stomatal exchange. 1: grass, 2: arable land, 3: permanent crops, 4: coniferous forest, 5: deciduous forest, 6: water, 7: urban, 8: other, 9: desert.**

land use	1	2	3	4	5	6	7	8	9
$f_{min}$ (-)	0.01	0.01	0.01	0.1	0.1	-999	-999	0.01	-999
$\alpha$ ( $\mu\text{mol m}^{-2} \text{s}^{-1}$ ) <sup>-1</sup>	0.009	0.009	0.009	0.006	0.006	-999	-999	0.009	-999
$\alpha$ ( $\text{W m}^{-2}$ ) <sup>-1</sup> (a)	0.0411	0.0411	0.0411	0.0274	0.0274	-999	-999	0.0411	-999
$T_{opt}$ (°C)	26	26	26	18	20	-999	-999	26	-999
$T_{min}$ (°C)	12	12	12	0	0	-999	-999	12	-999
$T_{max}$ (°C)	40	40	40	36	35	-999	-999	40	-999
$g_{max}$ ( $\text{mmol m}^{-2} \text{s}^{-1}$ )	270	300	300	140	150	-999	-999	270	-999
$g_{max}$ (m/s)	0.00659	0.00732	0.00732	0.00342	0.00366	-999	-999	0.00659	-999
$vpd_{max}$ (kPa)	1.3	0.9	0.9	0.5	1	-999	-999	1.3	-999
$vpd_{min}$ (kPa)	3	2.8	2.8	3	3.25	-999	-999	3	-999

(a) conversion  $\alpha$  ( $\text{W m}^{-2}$ )<sup>-1</sup> = 4.57  $\alpha$  ( $\mu\text{mol m}^{-2} \text{s}^{-1}$ )<sup>-1</sup> ;

(b) conversion  $g_{max}$  (m/s) =  $g_{max}(R T/P)$  ( $\text{mmol m}^{-2} \text{s}^{-1}$ ),  $R$  gas constant. For  $T=20$  °C,  $P=1$  atm.,  $R T/P \approx 1/41000$   $\text{mmol/m}^3$ .

Graphs of all correction factors and the resulting stomatal conductance, for different meteorological conditions, are shown in appendix E. Here also, a comparison has been made between the Emberson parameterization and those of Wesely (1989) and Baldocchi et al. (1987).

Within the stomata,  $\text{NH}_3$  is assumed to be in equilibrium with the apoplastic ammonium concentration. The theoretical stomatal compensation point,  $\chi_s$ , is calculated following Nemitz et al. (2001) and Wichink Kruit et al. (2007), analogously to the atmospheric ammonia concentration at the external leaf surface:

$$\chi_s = \frac{2.75 \cdot 10^{15}}{T_s + 273.15} \exp\left(\frac{-1.04 \cdot 10^4}{T_s + 273.15}\right) \cdot \Gamma_s, \quad (25)$$

where  $\chi_s$  is the stomatal compensation point (in  $\mu\text{g m}^{-3}$ ),  $T_s$  is the leaf surface temperature (in °C) and  $\Gamma_s$  is the dimensionless ratio between the apoplastic molar  $\text{NH}_4^+$  and  $\text{H}^+$  concentration.

A generalized equation that describes the annual trend in  $\Gamma_s$  as a function of the ‘long-term’  $\text{NH}_3$  concentration and the leaf surface temperature is derived by Wichink Kruit et al. (2010):

$$\Gamma_s(T_s) = \Gamma_{s,micromet} \cdot 4.7 \cdot \exp(-0.071 \cdot T_s) \quad (26)$$

where  $\Gamma_{s,micromet} = 362 \cdot \chi_{a,4m('long-term')}$  derived from micrometeorological measurements for the single-layer canopy compensation point model and  $\chi_{a,4m('long-term')}$  is the ‘long-term’ atmospheric  $\text{NH}_3$  concentration at four meters height. The functional behaviour of the compensation point as function of atmospheric  $\text{NH}_3$  concentration and temperature is shown in Appendix F.

## 7 Exchange in case of snow

In case of snow, the above parameterizations are not used; instead there is one overall canopy resistance:

$$\begin{aligned} R_c &= 500 \text{ s m}^{-1} & , T < -1 \text{ }^\circ\text{C}; \\ R_c &= 70 (2-T) \text{ s m}^{-1} & , -1 \text{ }^\circ\text{C} \leq T \leq 1 \text{ }^\circ\text{C} \\ R_c &= 70 \text{ s m}^{-1} & , T > 1 \text{ }^\circ\text{C}. \end{aligned} \tag{27}$$



## References

- Asman, W.A.H. (1994) Emission and deposition of ammonia and ammonium. *Nova Acta Leopoldina* NF 70, Nr. 288: 263-297.
- Baldocchi, D.D., B.B. Hicks and P. Camara (1987) A canopy stomatal resistance model for gaseous deposition to vegetated surfaces. *Atmospheric Environment* 21: 91-101.
- Boer, M. de, J. de Vente, C.A. Múcher, W. Nijenhuis and H.A.M. Thunnissen (2000) An approach towards pan-European land cover classification and change detection, NRSP-2, Report 00-18, Delft.
- EEA, 2000. Documentation about the Corine landcover 2000 dataset is available from: <http://reports.eea.europa.eu/COR0-landcover>.
- Emberson, L.D., M.R. Ashmore, D. Simpson, J.-P. Tuovinen and H.M. Cambridge (2000a) Towards a model of ozone deposition and stomatal uptake over Europe. EMEP/MSC-W 6/2000, Norwegian Meteorological Institute, Oslo.
- Emberson, L.D., M.R. Ashmore, D. Simpson, J.-P. Tuovinen and H.M. Cambridge (2000b) Modelling stomatal ozone flux across Europe. *Water, Air and Soil Pollution* 109: 403-413.
- Erismann, J.W. and W.A.J. van Pul (1994) Parameterization of surface resistance for the quantification of atmospheric deposition of acidifying pollutants and ozone. *Atmospheric Environment* 16: 2595-2607.
- Jaarsveld, J.A. van (2004) The Operational Priority Substances model. Description and validation of OPS-Pro 4.1. Report 500045001. RIVM, Bilthoven.
- Jarvis, P.G. (1976) The interpretation of the variations in leaf water potential and stomatal conductance found in canopies in the field. *Philosophical Transactions of the Royal Society of London, Series B*, 273: 593- 610.
- Milford, C., K.J. Hargreaves and M.A. Sutton (2001b) Fluxes of NH<sub>3</sub> and CO<sub>2</sub> over upland moorland in the vicinity of agricultural land. *Journal of Geophysical Research* 106: 24169-24181.
- Monteith, J.L. (1973) *Principles of Environmental Physics*. Edward Arnold, London.
- Nemitz, E., C. Milford C. and M.A. Sutton (2001) A two-layer canopy compensation point model for describing bi-directional biosphere-atmosphere exchange of ammonia. *Quarterly Journal of the Royal Meteorological Society* 127: 815-833.
- Norman, J.M. (1982) Simulation of microclimates. In: Hatfield, J.L. and I.J. Thomason (Eds.), *Biometeorology in Integrated Pest Management*. Academic Press, New York, pp. 65-99.
- Pul, W.A.J. van and A.F.G. Jacobs (1994) The conductance of a maize crop and the underlying soil to ozone under various environmental conditions. *Boundary Layer Meteorology* 69: 83-99.



- Pul, W.A.J. van, M.M.P. van den Broek, H. Volten, A. van der Meulen, A.J.C. Berkhout, K.W. van der Hoek, R.J. Wichink Kruit, J.F.M. Huijsmans, J.A. van Jaarsveld, B.J. de Haan en R.B.A. Koelemeijer (2008) Het ammoniakgat: onderzoek en duiding. Report 680150002. RIVM, Bilthoven.
- Schaap, M., R.M.A. Timmermans, M. Roemer, G.A.C. Boersen, P.J.H. Bultjes, F.J. Sauter, G.J.M. Velders and J.P. Beck (2008) The LOTOS–EUROS model: description, validation and latest developments, *Int. J. Environment and Pollution*, Vol. 32, No. 2: 270–290.
- Simpson, D., H. Fagerli, J.E. Jonson, S. Tsyro, P. Wind and J.P. Tuovinen (2003) Transboundary acidification, eutrophication and ground level ozone in Europe, Part I, EMEP status report.
- Simpson, D. (2008) Data from input files for EMEP model: Inputs\_DO3SE.csv, Inputs\_LandDefs.csv (parameters for land use and stomatal resistance modelling), originally based upon ideas/data in Emberson (2000a); updated to take account of forest-group meeting of Rome, 6-7th Dec. 2007 (L. Emberson, Chair) and of Revisions to Mapping Manual, 2007 (<http://www.icpmapping.org/>)
- Sutton, M.A. and D. Fowler D. (1993) A model for inferring bi-directional fluxes of ammonia over plant canopies. Proceedings of the WMO Conference on the Measurement and Modelling of Atmospheric Composition Changes Including Pollution Transport. WMO/GAW-91, WMO Geneva, pp 179-182.
- Sutton, M. A., J.K. Burkhardt, D. Guerin, E. Nemitz and D. Fowler (1998) Development of resistance models to describe measurements of bi-directional ammonia surface-atmosphere exchange, *Atmospheric Environment* 32: 473-480.
- Velders, G.J.M., J.M.M. Aben, J.A. van Jaarsveld, W.A.J. van Pul, W.J. de Vries, M.C. van Zanten (2010) Grootchalige stikstofdepositie in Nederland. Analyse bronbijdragen op provinciaal niveau. Report 500088007. RIVM, Bilthoven.
- Weiss, A. and J.M. Norman (1985) Partitioning solar radiation into direct and diffuse, visible and near-infrared components. *Agric. Forest Meteorol.* 34: 205-213.
- Wesely, M.L. (1989) Parameterization of surface resistances to gaseous dry deposition in regional scale numerical models. *Atmospheric Environment* 23: 1293-1304.
- Wichink Kruit, R.J., W.A.J. van Pul, R.P. Otjes, P. Hofschreuder, A.F.G. Jacobs and A.A.M. Holtslag (2007) Ammonia fluxes and derived canopy compensation points over non-fertilized agricultural grassland in The Netherlands using the new gradient ammonia - high accuracy - monitor (GRAHAM). *Atmospheric Environment* 41: 1275-1287.
- Wichink Kruit, R.J., W.A.J. van Pul, F.J. Sauter, M. van den Broek, E. Nemitz, M.A. Sutton, M. Krol and A.A.M. Holtslag (2010) Modeling the surface-atmosphere exchange of ammonia. *Atmospheric Environment*, Vol. 44, 7: 877-1004.
- Zhang L., M.D. Moran and J.R. Brook (2001) A comparison of models to estimate in-canopy photosynthetically active radiation and their influence on canopy stomatal resistance *Atmospheric Environment* 35: 4463–4470.

## Appendix A. Description of DEPAC v3.3

Version 3.3 of DEPAC contains the original parameterizations for calculating the canopy resistance  $R_c$  as described in Erisman et al. (1994) and Appendix I in Van Jaarsveld (2004). Compared to the original DEPAC, the code of version 3.3 has been restructured and better documented. The text below is an integral copy of the relevant sections of this appendix, for the full text we refer the reader to Van Jaarsveld (2004). A few differences exist between the description and the actual code; those are added in the text.

### The canopy resistance

The canopy resistance  $R_c$  may be considered as the result of a number of sub-resistances representing different processes in and at the canopy. The general model with the canopy resistance split up in sub-resistances is given in Figure 2.

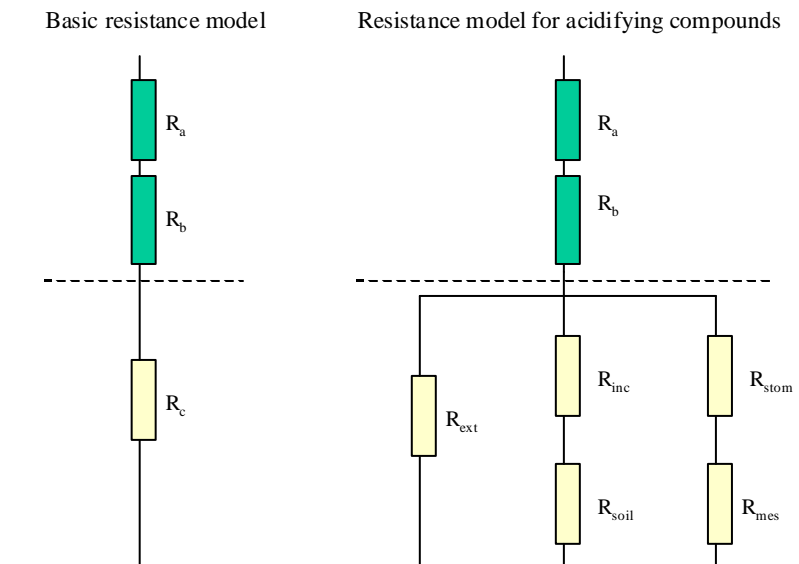


Figure 2. Resistance model with sub-resistances for the canopy resistance  $R_c$ .

In this model  $R_{stom}$  and  $R_{mes}$  represent the stomatal and mesophyll resistances of leaves respectively.  $R_{inc}$  and  $R_{soil}$  are resistances representing in-canopy vertical transport to the soil, which bypasses leaves and branches.  $R_{ext}$  is an external resistance, which represents transport via leaf and stem surfaces, especially when these surfaces are wet. The (effective) canopy resistance  $R_c$  can be calculated as:

$$R_c = \frac{1}{\frac{1}{R_{stom} + R_{mes}} + \frac{1}{R_{inc} + R_{soil}} + \frac{1}{R_{ext}}} \quad \text{A.1.}$$

The DEPAC module contains parameters for each of the resistances given in Figure 2 for various land-use types and for each of the gaseous components. Furthermore, a seasonal distinction is made in the values of some of the resistances. In a number of cases the general resistance model reduces to its most basic form, that is, when detailed information is lacking (e.g. for HNO<sub>3</sub>) or when the surface is non-vegetative such as for bare soil, water surfaces, buildings or when there is a snow-cover. In these cases only  $R_{soil}$  determines the effective canopy resistance, because  $R_{ext}$  and  $R_{stom}$  are set to (near) infinity.

$$\begin{aligned} \text{Water surface: } R_c &= R_{soil} = R_{water}; \\ \text{Bare soil: } R_c &= R_{soil}; \\ \text{Snow cover: } R_c &= R_{soil} = R_{snow}; \\ \text{HNO}_3 R_c &= R_{soil}. \end{aligned}$$

### Stomatal resistance

$R_{stom}$  is calculated according to Wesely (1989):

$$R_{stom,H_2O} = R_i \cdot \left[ 1 + \left( \frac{200}{Q + 0.1} \right)^2 \right] \cdot \frac{400}{T_s \cdot (40 - T_s)} \quad \text{A.2.}$$

and

$$R_{stom,x} = R_{stom,H_2O} \cdot \frac{D_{H_2O}}{D_x} \quad \text{A.3.}$$

where  $Q$  is the global radiation in  $\text{W m}^{-2}$ ,  $T_s$  the surface temperature in  $^{\circ}\text{C}$ ,  $D_{H_2O}$  the molecular heat diffusivity of water vapour and  $D_x$  the molecular heat diffusivity of the substance, both in  $\text{m}^2 \text{s}^{-1}$ .

$R_i$  values are given in Table 2. Values of -999 in this and further tables indicate that the resistance is near infinity and plays no role under the given conditions.

**Table 2.  $R_i$  values at different conditions according to Wesely (1989) (in  $\text{s m}^{-1}$ ).**

Season	Grass land	Arable land	Permanent crops	Coniferous forest	Deciduous forest	Water	Urban	Other grassy area	Desert
Summer	60	60	60	130	70	-999	-999	60	-999
Autumn	-999	-999	-999	250	-999	-999	-999	-999	-999
Winter	-999	-999	-999	400	-999	-999	-999	-999	-999
Spring	120	120	120	250	140	-999	-999	120	-999

### Mesophyll resistance

The mesophyll resistance  $R_m$  is set at  $0 \text{ s m}^{-1}$  for all circumstances because there are indications that it is low for substances as SO<sub>2</sub>, O<sub>3</sub> and NH<sub>3</sub> and because of lack of relevant data to justify other values (Wesely, 1989).

### In-canopy resistance

$R_{inc}$  represents the resistance against turbulent transport within the canopy and is calculated according to Van Pul and Jacobs (1994):

$$R_{inc} = \frac{b \cdot LAI \cdot h}{u_*} \quad \text{A.4.}$$

- + where  $b$  is an empirical constant ( $14 \text{ m}^{-1}$ ),  $h$  the height of the vegetation in m (1 m for arable land and 20 m for forests) and  $LAI$  the Leaf Area Index (dimensionless). The authors themselves qualify Equation A.4. as still preliminary. DEPAC uses LAI as a function of the time of the year according to Table 3. The calculation of  $R_{inc}$  according to Eq. A.4. is only carried out for arable land and forest. For all other land-use classes  $R_{inc}$  is set at 0. Note, in current code version 3.3 is  $R_{inc}$  not only calculated for arable land and forests, but for permanent crops as well.

**Table 3. Leaf Area Indexes for some land-use classes.**

	Grass	Arable land	Perm. Crops*	Conif. forest	Decid. Forest	Water	Urban	Other grassy area\$	Desert
May and October	6	1.25	1.25	5	1.25	N/A	N/A	6	N/A
June and September	6	2.5	2.5	5	2.5	N/A	N/A	6	N/A
July and August	6	5	5	5	5	N/A	N/A	6	N/A
November - April	6	0.5	0.5	5	0.5	N/A	N/A	6	N/A

\* The LAI of permanent crops is taken equal to the LAI of arable land. In the original Table in Van Jaarsveld (2004) LAI values were given as N/A.

\$ The LAI of other grassy area is taken equal to the LAI of grass. In the original Table in Van Jaarsveld (2004) LAI values were given as N/A.

### Soil resistance

DEPAC uses  $R_{soil}$  values as given in Table 4. The general effect is that wet surfaces enhance the uptake of (soluble) gases. If the soil is frozen and/or covered with snow then the uptake is much less.

**Table 4. Soil resistances in  $\text{s m}^{-1}$  for various substances. The values apply to all land-use types including urban areas.**

	$R_{soil\_wet}$	$R_{soil\_dry}$	$R_{soil\_frozen}^{\&}$	$R_{water}$	$R_{snow}$
SO <sub>2</sub>	10	1000	500	10	$70(2-T)^{\$}$
NO <sub>2</sub>	2000	1000	2000	2000	2000
NO	-999	-999**	-999	2000	2000
HNO <sub>3</sub>	10	10	10	10	$50^{\#}$
NH <sub>3</sub>	10	100**	1000	10	$70(2-T)^{\$}$

& if  $T < -1^{\circ}\text{C}$ .

# only if  $T < -5^{\circ}\text{C}$ , otherwise  $R_{snow} = 10 \text{ s m}^{-1}$ .

\$ minimal value = 70; if  $T < -1^{\circ}\text{C}$ ,  $R_{snow} = 500 \text{ s m}^{-1}$ .

\*\* In current code version 3.3  $R_{soil\_dry}$  for NO and NH<sub>3</sub> for land use class urban is set to  $1000 \text{ s m}^{-1}$ .

**External resistance**

The external resistance  $R_{ext}$  represents a sink for gases through external leaf uptake and is especially important for soluble gases at wet surfaces. Under some conditions the external leaf sink can be much larger than the stomatal uptake.  $R_{ext}$  is only calculated for grass, arable land and forest land-use types.

**SO<sub>2</sub>**

The following empirical expressions from Erisman et al. (1994) are used for SO<sub>2</sub>:

During or just after precipitation (*wet* = true):

$$R_{ext} = 10 \text{ s m}^{-1}$$

In all other cases:

$$\text{if } T > -1 \text{ } ^\circ\text{C:} \quad R_{ext} = 25000 \cdot e^{-0.0693rh} \quad \text{if } rh < 81.3 \%$$

$$R_{ext} = 10 + 0.58 \cdot 10^{12} \cdot e^{-0.278rh} \quad \text{if } rh > 81.3 \%$$

$$\text{if } -1 > T > -5 \text{ } ^\circ\text{C:} \quad R_{ext} = 200 \text{ s m}^{-1}$$

$$\text{if } T < -5 \text{ } ^\circ\text{C:} \quad R_{ext} = 500 \text{ s m}^{-1}.$$

Here, *rh* expresses the relative humidity in %.

**NO<sub>2</sub>**

Under all conditions  $R_{ext} = 2000 \text{ s m}^{-1}$ .

**NO**

Under all conditions  $R_{ext} = 10000 \text{ s m}^{-1}$ .

**HNO<sub>3</sub>**

The basic resistance model is applied and thus  $R_{ext}$  is not required.

## Appendix B. Land use and leaf area index

The deposition module DEPAC uses nine land use classes:

1. rass
2. arable land
3. permanent crops
4. coniferous forest
5. deciduous forest
6. water
7. urban
8. other, i.e. short grassy area
9. desert.

The leaf area index (LAI) is the one-sided leaf area per m<sup>2</sup> earth surface. Since the choice of LAI-parameterization in DEPAC v.3.3 (Van Jaarsveld, 2004) was not well documented, it was decided to compare these parameterizations to those used in the EMEP model (Emberson, 2000a):

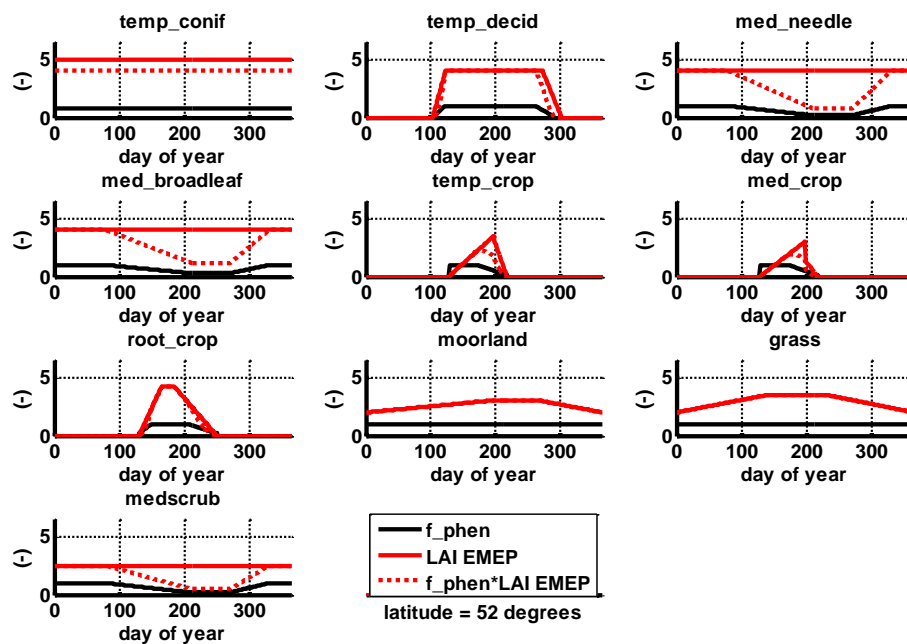


**Figure 3.** Leaf area index and correction factor for phenology (reducing the stomatal conductance) during a year for EMEP land use types.

It was decided to use EMEP's parameterization for LAI in the updated DEPAC module for several reasons:

- it looks more realistic;
- it is better supported by literature;
- it has a better representation of the growing season (e.g. latitude dependent start and end of growing season).

From the above figure, we see that the growing season for *temp\_crop* (wheat or barley) and *med\_crop* (maize) is very short and it was decided to use the *LAI* for *root\_crop* for both arable land and permanent crop. Other parameters for the stomatal conductance are used as in *temp\_crop*. The DEPAC land use class *other* uses the *LAI* and stomatal parameters from land use class *grass*.

**Table 5. Translation from DEPAC land use classes to EMEP.**

DEPAC	LAI from EMEP Land use classification	Stomatal conductance parameters from EMEP land use classification
1   grass	Grass	grass
2   arable land	root crops	temperate crops
3   permanent crops	root crops	temperate crops
4   coniferous forest	temperate/boreal coniferous forest	temperate/boreal coniferous forest
5   deciduous forest	temperate/boreal deciduous forest	temperate/boreal deciduous forest
6   water	Water	water
7   urban	Urban	urban
8   other	Grass	grass
9   desert	Desert	desert

DEPAC v.3.11 makes a distinction between the leaf area index, which is used for the stomatal resistance and the surface area index, ( $SAI = LAI +$  area index of stems and branches), which is used for the external resistance.

The following function is used to describe the temporal behavior of the leaf area index:

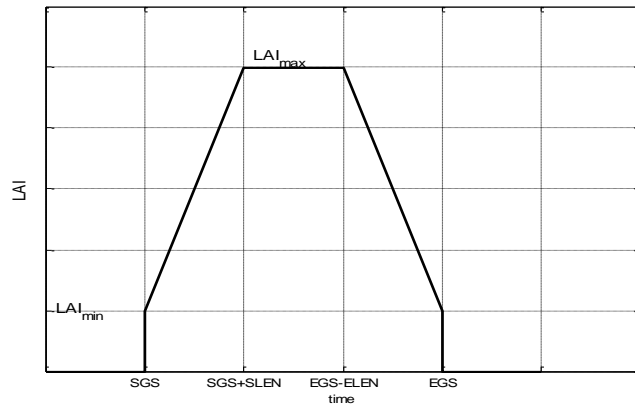


**Figure 4. Leaf area index as function of time. SGS: start growing season; EGS: end growing season; SLEN: length of starting phase of growing season; ELEN: length of end phase of growing season.**

The start and end of growing season (SGS and EGS resp.) are dependent of the latitude  $\lambda$  (in degrees):

$$SGS(\lambda) = SGS(50) + \Delta_{SGS} (\lambda - 50.0)$$

$$EGS(\lambda) = EGS(50) + \Delta_{EGS} (\lambda - 50.0).$$

Values of  $SGS(50)$ ,  $EGS(50)$ ,  $\Delta_{EGS}$ ,  $\Delta_{SGS}$ ,  $SLEN$  and  $ELEN$  are given in Table 6. The surface area index as function of LAI is shown in Table 7.

**Table 6. Parameters for leaf area index from Emberson (2000a).**

land use class		SG	$\Delta_{SGS}$	EGS(50)	$\Delta_{EGS}$	LAI <sub>MIN</sub>	LAI <sub>MAX</sub>	SLEN	ELEN
Emberson	DEPAC	S(50)							
grass	grass	0	0.0	366	0.0	2.0	3.5	140	135
root_crop	arable_land	130	0.0	250	0.0	0.0	4.2	35	65
root_crop	permanent_crops	130	0.0	250	0.0	0.0	4.2	35	65
temp_conif	coniferous_forest	0	0.0	366	0.0	5.0	5.0	1	1
temp_decid	deciduous_forest	100	1.5	307	-2.0	0.0	4.0	20	30
water	water	-999	-999	-999	-999	-999	-999	-999	-999
urban	urban	-999	-999	-999	-999	-999	-999	-999	-999
grass	other	0	0.0	366	0.0	2.0	3.5	140	135
desert	desert	-999	-999	-999	-999	-999	-999	-999	-999

**Table 7. Surface area index as function of LAI (Simpson et al., 2003).**

Land use class DEPAC	SAI
grass	LAI
arable_land	LAI, outside growing season max((5/3.5)·LAI, LAI + 1.5), starting phase of growing season LAI + 1.5, maximal and end phase of growing season
permanent_crops	LAI + 0.5 <sup>\$</sup>
coniferous_forest	LAI + 1
deciduous_forest	LAI + 1
water	-
urban	-
other	LAI
desert	-

\$: not specified in EMEP report

In Figure 5, a comparison has been made between the EMEP and DEPAC v.3.3 parameterizations for LAI using Table 5. In the same figure, the surface area index SAI and the phenology correction factor  $f_{phen}$  for the stomatal conductance is shown. Input data are from Simpson, 2008.



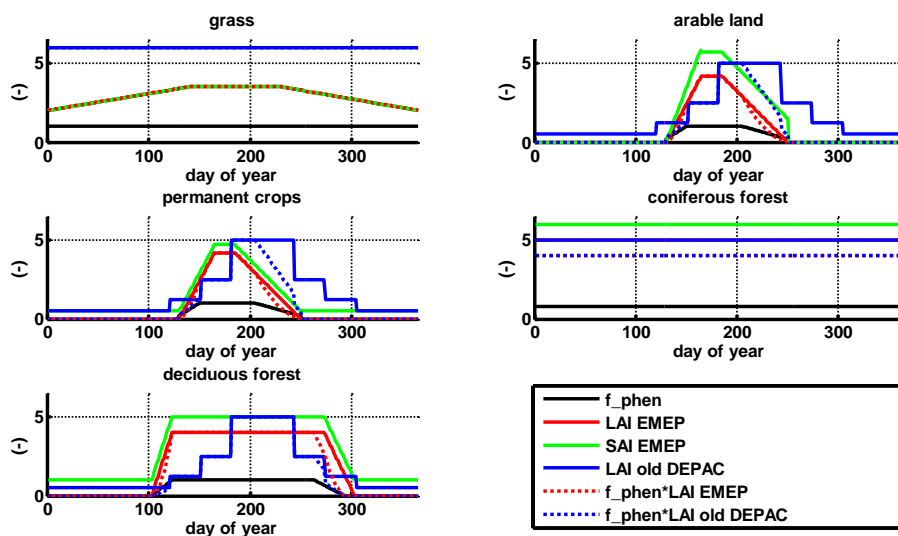


Figure 5. Leaf area index LAI, surface area index SAI and phenology factor  $f_{phen}$  during a year for different land use types, latitude = 52 degrees North. EMEP's parameterization compared to DEPAC v.3.3. For coniferous forest, the LAI for EMEP and DEPAC v.3.3 is the same.

Since the factor  $f_{phen}$  does not have much influence for the land use types currently used in DEPAC, it was decided to ignore this factor. The extra factor available in the EMEP code that reduces LAI for latitudes above 60° North, has also not been included.

**Extension of land use classes.**

If the number of land use classes in DEPAC is extended, all parameters depending on the *lu*-value have to be set. The following table lists those parameters.

<b>LAI_par</b>	
sgs50	growing season at 50 degrees latitude (days)
dsgs	shift in start growing season (days/degree latitude)
egs50	end growing season at 50 degrees latitude (days)
degs	shift in end growing season (days/degree latitude),
laimin	leaf area index at start and end of growing season (m <sup>2</sup> leaf/m <sup>2</sup> ground surface)
laimax	maximal leaf area index (m <sup>2</sup> leaf/m <sup>2</sup> ground surface)
s_lai_len	length of starting phase of LAI (days)
e_lai_len	length of end phase of LAI (days)
<b>Rc_stom</b>	
F_min	
alpha	
Topt	
Tmin	
Tmax	
g_max	
vpd_max	
vpd_min	
<b>R_inc</b>	
b	empirical constant with value 14 or NaN (-999)
h	vegetation height [m]
<b>Compensation punt</b>	
gamma_stom_c_fac	factor in linear relation between $\Gamma_{stom}$ and NH <sub>3</sub>
gamma_soil_c_fac	the same for soil, currently only specified for water
<b>Rsoil</b>	= 100 s/m, except $R_{soil} = 10$ s/m, for $lu = 6$
<b>z0_lu</b>	$z_0$ for each $lu$ (set in modvar)

## Appendix C. Radiation model Weiss and Norman

In order to compute the influence of solar radiation on the stomata, a simple radiation model has been employed. First we repeat some definitions from the American Meteorological Society (<http://amsglossary.allenpress.com/glossary>):

**solar radiation**—The total electromagnetic radiation emitted by the sun. ... About one-half of the total energy in the solar beam is contained within the visible spectrum from 0.4 to 0.7  $\mu\text{m}$ , and most of the other half lies in the near-infrared, a small additional portion lying in the ultraviolet.

**global radiation**—Solar radiation, direct and diffuse, received from a solid angle of  $2\pi$  steradians on a horizontal surface.

**direct solar radiation**—Solar radiation that has not been scattered or absorbed.

In practice, solar radiation that has been scattered through only a few degrees, characteristic of the diffraction peak of the scattering function, is unavoidably included in the operational measurement of direct solar radiation by a pyrheliometer.

**diffuse sky radiation**—Solar radiation that is scattered at least once before it reaches the surface.

As a percentage of the global radiation, diffuse radiation is a minimum, less than 10% of the total, under clear sky conditions and overhead sun. The percentage rises with increasing solar zenith angle and reaches 100% for twilight, overcast, or highly turbid conditions. It is measured by a shadow band pyranometer.

**total solar irradiance**—(Abbreviated TSI.) The amount of solar radiation received outside the earth's atmosphere on a surface normal to the incident radiation, and at the earth's mean distance from the sun. Reliable measurements of solar radiation can only be made from space and the precise record extends back only to 1978. The generally accepted value is  $1368 \text{ W m}^{-2}$  with an accuracy of about 0.2%. Variations of a few tenths of a percent are common, usually associated with the passage of sunspots across the solar disk. The solar cycle variation of TSI is on the order of 0.1%.

We follow Weiss and Norman (1985), the notation is however somewhat different.

Characters  $Q$ ,  $R$  and  $S$  are used for the radiation parameters in the radiation model:

- $Q$  : solar irradiance, on a surface normal to the incoming sun beams ( $\text{W/m}^2$ );
- $R$  : potential radiation on a horizontal surface ( $\text{W/m}^2$ ); *potential* means that it occurs only in clear sky conditions;
- $S$  : actually occurring (measured) radiation on a horizontal surface; this type of radiation includes the influence of clouds ( $\text{W/m}^2$ ).

The following subscripts are used:

- $vis$  : visual;
- $ni$  : near-infrared;
- $dir$  : direct;
- $diff$  : diffuse.

We start with the solar irradiance at the top of the atmosphere, according to Weiss and Norman (1985):

$$Q_{TSI} : \text{total solar irradiance} = 1320 \text{ W/m}^2. \quad \text{C.1.}$$

The solar irradiance is split into a part in the visible wave band and a part in the near-infrared (the ultra-violet part is neglected):

$$Q_{vis} = \alpha_{vis} Q_{TSI}, \quad Q_{ni} = \alpha_{ni} Q_{TSI}, \quad \text{C.2.}$$

$\alpha_{vis}$  : fraction of radiation in the visible wave band = 0.46;

$\alpha_{ni}$  : fraction of radiation in the near-infrared wave band =  $1 - \alpha_{vis}$ .

Weiss and Norman give the following parameterizations for direct and diffuse parts of visible radiation  $R_{vis,dir}$  and  $R_{vis,diff}$ :

$$R_{vis,dir} = Q_{vis} \exp\left(-K_{vis} \frac{P}{P_0} m\right) \cos \theta \quad \text{C.3.}$$

$$R_{vis,diff} = 0.4(Q_{vis} - R_{vis,dir}) \cos \theta \quad \text{C.4.}$$

with

$\theta$  : zenith angle;

$K_{vis}$  : extinction coefficient for visible radiation = 0.185;

$P$  : pressure;

$P_0$  : pressure at sea level (same dimension as  $P$ );

$m$  : optical air mass,  $m = (\cos \theta)^{-1}$ .

The 0.4 is the fraction of intercepted visible beam radiation that is converted to downward diffuse radiation at the surface.

For near-infrared radiation:

$$R_{ni,dir} = Q_{ni} \exp\left(-K_{ni} \frac{P}{P_0} m - w\right) \cos \theta \quad \text{C.5.}$$

$$R_{ni,diff} = 0.6(Q_{ni} - R_{ni,dir} - w) \cos \theta \quad \text{C.6.}$$

$K_{ni}$  : extinction coefficient for near-infrared radiation = 0.06;

$w$  : water absorption in the near infrared for 10 mm of precipitable water

$$w = Q_{TSI} 10^{\left[-1.1950 + 0.4459 \log_{10}(m) - 0.0344 [\log_{10}(m)]^2\right]}.$$

Adding direct and diffuse parts:  $R_{vis} = R_{vis,dir} + R_{vis,diff}$ ,  $R_{ni} = R_{ni,dir} + R_{ni,diff}$  and defining

$R_{total} = R_{vis} + R_{ni}$ , we have expressed all forms of potential radiation  $R$  in terms of known parameters and zenith angle  $\theta$ .

It is assumed that the ratio of visible and total radiation is the same for the potential radiation and for the actually occurring radiation. Total radiation  $S_{total}$  (in Weiss and Norman  $R_T$ ) is a quantity that is generally available as measurement or as a model result. The actually occurring visible radiation  $S_{vis}$  can now be estimated from the total radiation by:

$$\frac{S_{vis}}{S_{total}} = \frac{R_{vis}}{R_{total}} \text{ or } S_{vis} = \frac{S_{total}}{R_{total}} R_{vis} = \mathbf{RATIO} \cdot R_{vis} , \quad \text{C.7.}$$

with

$$\mathbf{RATIO} : \text{ratio of measured to potential solar radiation, } \mathbf{RATIO} = \frac{S_{total}}{R_{total}} .$$

The same holds for near-infrared:

$$S_{ni} = \mathbf{RATIO} \cdot R_{ni} . \quad \text{C.8.}$$

From an analysis of measurements by Weiss and Norman, they derived a relation for the fraction of direct radiation in the visible spectrum:

$$f_{vis,dir} \equiv \frac{S_{vis,dir}}{S_{vis}} = \frac{R_{vis,dir}}{R_{vis}} \left[ 1 - \left( \frac{A - \mathbf{RATIO}}{B} \right)^{2/3} \right] , \quad \text{C.9.}$$

and for the near-infrared:

$$f_{ni,dir} \equiv \frac{S_{ni,dir}}{S_{ni}} = \frac{R_{ni,dir}}{R_{ni}} \left[ 1 - \left( \frac{C - \mathbf{RATIO}}{D} \right)^{2/3} \right] \quad \text{C.10.}$$

with empirical coefficients  $A = 0.9$ ,  $B = 0.7$ ,  $C = 0.88$ ,  $D = 0.68$ . Note that  $f_{ni,dir}$  is not used here.

The fraction of diffuse radiation in the visible spectrum is

$$f_{vis,diff} = 1 - f_{vis,dir} . \quad \text{C.11.}$$

Now we can compute the direct and diffuse parts of the visible part of the measured radiation:

$$S_{vis,dir} = f_{vis,dir} S_{vis} \text{ and } S_{vis,diff} = f_{vis,diff} S_{vis} . \quad \text{C.12.}$$

Below, we show figures of radiation data of a test model; because measured radiation was not available, we used a cloud attenuation factor  $f_{cld}$  (between 0 and 1), simulating the effect of clouds:

$$S_{total} = f_{cld} R_{total} . \quad \text{C.13.}$$

In the following figures, we plot PAR (photoactive radiation), assuming that  $PAR = S_{vis}$ .

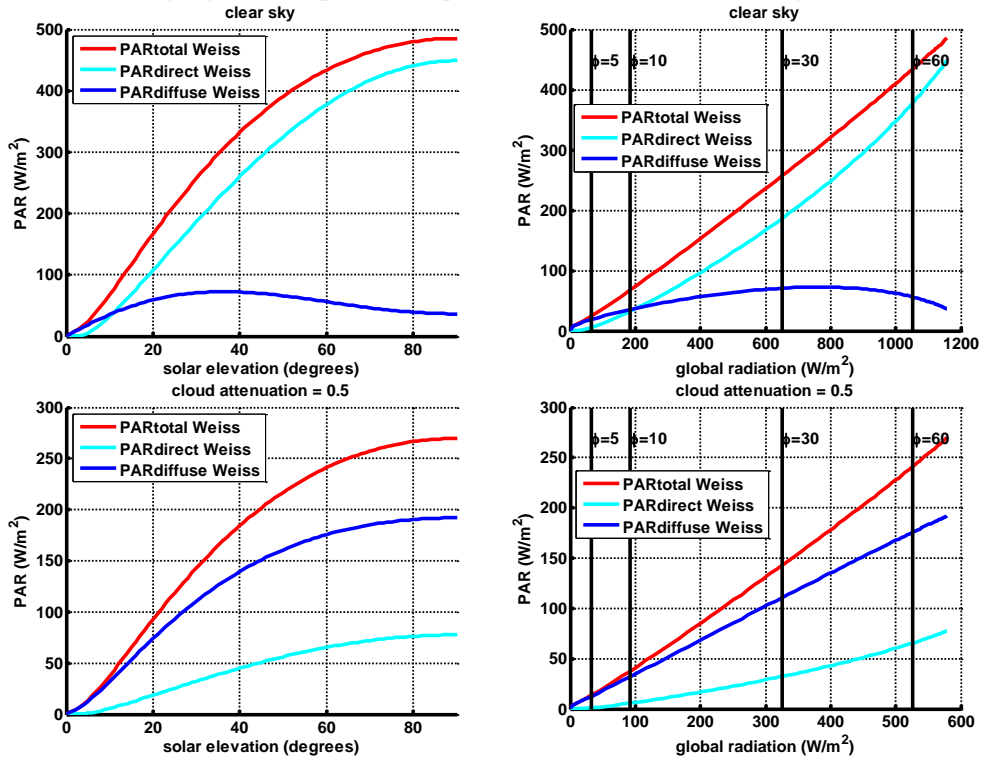


Figure 6. PAR (photoactive radiation) according to Weiss and Norman as function of the solar elevation  $\phi$  (left panels) and global radiation (right panels). Upper panels: clear sky conditions, lower panels: cloudy conditions (cloud attenuation factor = 0.5). Under cloudy conditions, there is more diffuse sun light than direct.

## Appendix D. Radiation/leaf model Norman and Zhang

Norman (1982) proposed the following parameterizations for radiation for sunlit leaves and shaded leaves in the canopy:

$$PAR_{shade} = PAR_{diffuse} \exp(-\frac{1}{2} LAI^{0.7}) + 0.07 PAR_{direct} (1.1 - 0.1 LAI) \exp(-\sin \phi) \quad D.1.$$

$$PAR_{sun} = \frac{PAR_{direct}}{2 \sin \phi} + PAR_{shade}, \quad D.2.$$

$PAR$  : photoactive radiation ( $W/m^2$ ) = radiation in visible spectrum =  $S_{vis}$  in Appendix C;

$LAI$  : leaf area index ( $m^2$  leaf /  $m^2$  surface);

$\phi$  : solar elevation ( $= \pi/2$  - zenith angle).

Note that  $PAR_{total} = PAR_{direct} + PAR_{diffuse}$  is the amount of energy that falls on  $1 m^2$  of earth surface, whereas  $PAR_{sun}$  is the amount of energy that falls on all sunlit leaves that are above  $1 m^2$  of earth surface.

Zhang (2001) modifies these expressions for  $LAI > 2.5$  and global radiation  $> 200 W/m^2$ :

$$PAR_{shade} = PAR_{diffuse} \exp(-\frac{1}{2} LAI^{0.8}) + 0.07 PAR_{direct} (1.1 - 0.1 LAI) \exp(-\sin \phi) \quad D.3.$$

$$PAR_{sun} = \frac{(PAR_{direct})^{0.8} \cos \alpha_1}{\sin \phi} + PAR_{shade}, \quad D.4.$$

with  $\alpha_1$  the angle between the leaf and the sun;  $\alpha_1$  has a value of  $60^\circ$  for a canopy assumed to have a spherical leaf angle distribution ( $\cos(\alpha_1) = 1/2$ ).

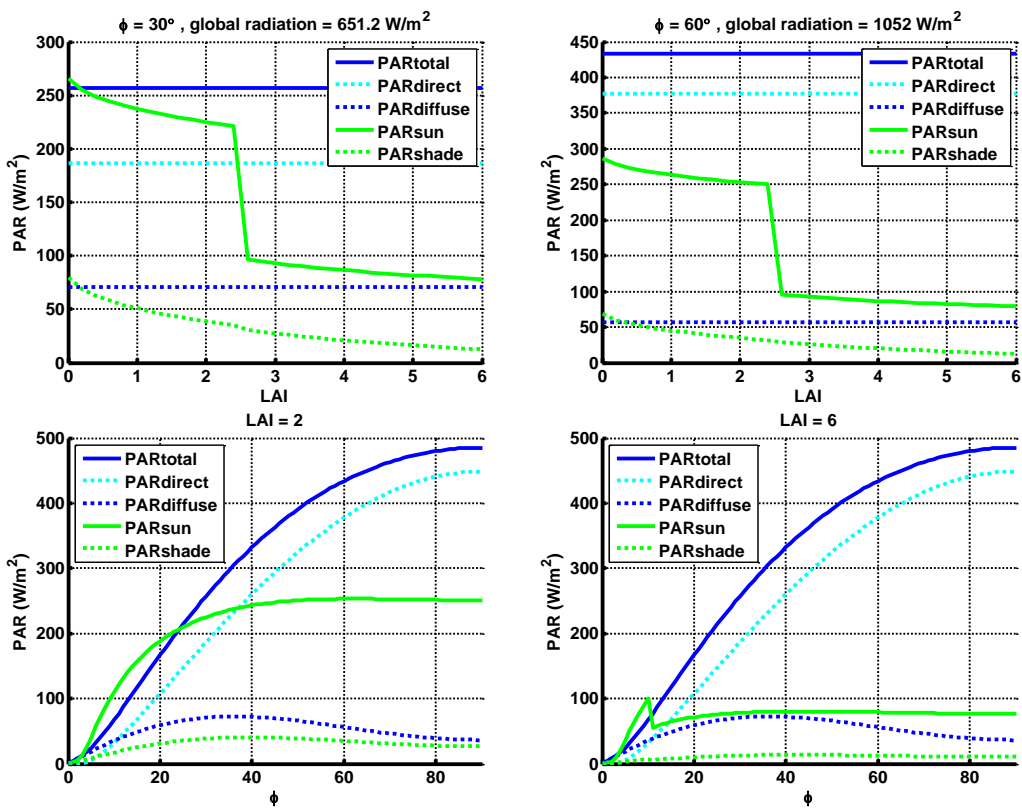


Figure 7. Different forms of PhotoActive Radiation PAR as a function of the leaf area index LAI (upper panels for solar elevation  $\phi = 30^\circ$  or  $60^\circ$ ) or as function of solar elevation  $\phi$  (lower panels for LAI = 2 or 6). For dense canopies (high LAI), there is less PAR available than for more open canopies.

The leaf area index for sunlit and shaded leaves is

$$LAI_{sun} = 2 \sin \phi \left[ 1 - \exp\left(-\frac{LAI}{2 \sin \phi}\right) \right], \quad LAI_{shade} = LAI - LAI_{sun}. \quad D.5.$$

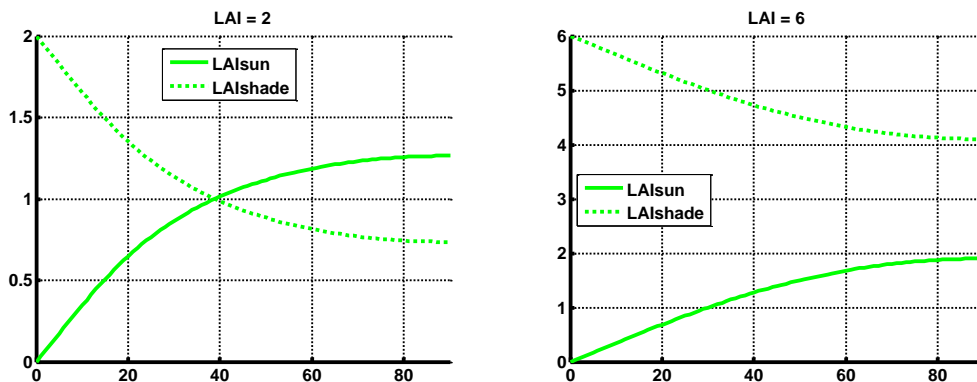


Figure 8. Leaf area indices for sunlit and shaded leaves as function of solar elevation for LAI = 2, 6. For dense canopies (high LAI), there is relatively more shade.



The correction factor  $f_{PAR}$  for the influence of the sun's radiation on the stomatal resistance is a weighted average of the corrections for sunlit and shaded leaves:

$$f_{PAR,sun} = [1 - \exp(-\alpha PAR_{sun})], \quad f_{PAR,shade} = [1 - \exp(-\alpha PAR_{shade})] \quad D.6.$$

$$f_{PAR} = \frac{LAI_{sun}}{LAI} f_{PAR,sun} + \frac{LAI_{shade}}{LAI} f_{PAR,shade}, \quad f_{PAR} = \max(f_{PAR}, f_{min}) \quad D.7.$$

with

$\alpha$  : species-specific parameter in light correction factor ( $[W/m^2]^{-1}$ );

$f_{min}$  : lower bound for correction factor (-).

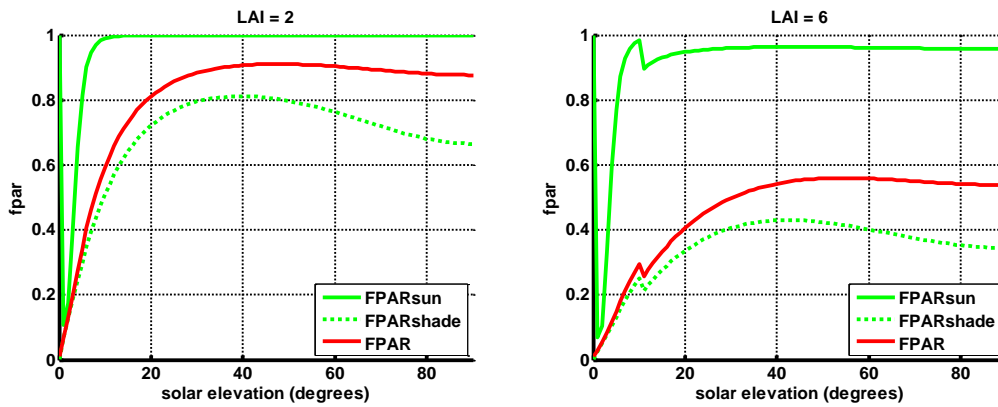


Figure 9. Correction factors  $f_{par}$  for sunlit and shaded leaves as function of solar elevation for LAI = 2 and 6 ( $f_{par} = 0$ : stomatal pathway closed;  $f_{par} = 1$ : no restriction due to PAR for stomatal exchange). For dense canopies (high LAI), the stomatal pathway is more restricted than for more open canopies, due to relatively more shaded leaves and less PAR.



## Appendix E. Stomatal resistance

In old DEPAC versions, two different parameterizations for the stomatal resistance were available: Baldocchi et al. (1987) and Wesely (1989). In the updated DEPAC version, another parameterization has been added: Emberson (2000a,b). We will evaluate here the differences between these three methods.

Note that the implementation of Baldocchi available in DEPAC does not include all features of the article of Baldocchi et al. (1987). In particular it does not use the vapour pressure deficit and it does not distinguish between sunlit and shaded leaves. Therefore, results of this implementation are denoted with  $\approx$ Baldocchi in the following figures. Furthermore, the implementation of Baldocchi in DEPAC contained errors, see Appendix H. These errors have been corrected for the tests in this report. Parameterizations shown here, are formulated in terms of conductance  $G=1/R$ . With a lower case  $g$  we denote leaf conductance, upper case  $G$  is used for a canopy averaged conductance.

All three parameterizations use a maximal stomatal conductance (for certain optimal conditions) that is reduced by different correction factors (between 0 and 1):

$$G_s = G_s^{\max} \cdot f_{phen} \cdot f_{vpd} \cdot f_T \cdot f_{PAR}, \quad \text{E.1.}$$

with

$G_s$  : canopy averaged stomatal conductance (m/s);

$G_s^{\max}$  : canopy averaged stomatal conductance for optimal conditions (m/s);

$f_{phen}$  : correction factor for phenology (-);

$f_{vpd}$  : correction factor for vapour pressure deficit (-);

$f_T$  : correction factor for temperature (-);

$f_{PAR}$  : correction factor for photoactive radiation (-).

Not all factors are used by all parameterizations and different expressions for the correction factors are used by Wesely, Baldocchi and Emberson.

Baldocchi and Emberson provide values for the maximal leaf conductance  $g_{s,ref}^{\max}$  for a reference gas (Baldocchi: water vapour, Emberson: ozone), that is constant over the year; they have to be multiplied by the leaf area index LAI to obtain a canopy conductance:

$$G_{s,ref}^{\max} = LAI \cdot g_{s,ref}^{\max} \quad \text{E.2.}$$

In this way a season dependency is built in, by means of the LAI, see Appendix B. Wesely directly gives values for the maximal canopy conductance  $G_{s,ref}^{\max}$  for water vapour that are season dependent. In order to obtain the maximal stomatal conductance for another gas than the reference, we multiply with the ratio of the diffusion coefficients:

$$G_s^{\max} = \frac{D}{D_{ref}} G_{s,ref}^{\max}, \quad \text{E.3.}$$

$D$  : diffusion coefficient of gas ( $m^2/s$ );  $D_{ref}$  : diffusion coefficient of reference gas ( $m^2/s$ ).

Values of canopy averaged maximal stomatal conductance for ammonia in the month July (maximal LAI) are shown in Figure 10. For water, urban and desert the stomatal conductance is 0 m/s. Translation from DEPAC land use classes to EMEP, following Table 5 in Appendix B.

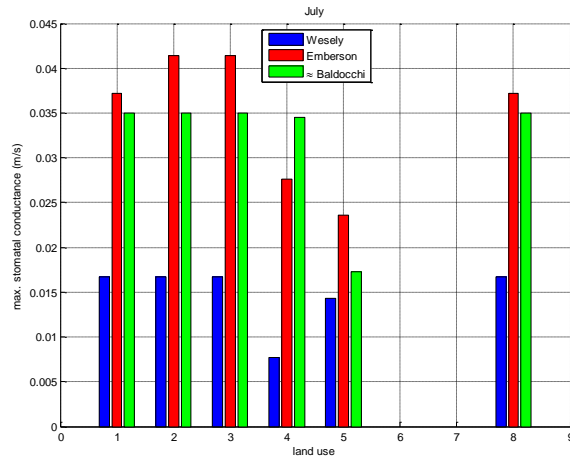


Figure 10. Canopy averaged maximal stomatal conductance for ammonia (m/s). 1 = grass, 2 = arable land, 3 = permanent crops, 4 = coniferous forest, 5 = deciduous forest, 6 = water, 7 = urban, 8 = other, 9 = desert.

Formulas for the other correction factors can be found in chapter 6.

The correction factor for vapour pressure deficit, which is used in the Emberson parameterization, is shown in Figure 11. Baldocchi has the option to use a correction factor for vapour pressure deficit, but in the current implementation this factor is not used. Wesely does not use the vapour pressure deficit.

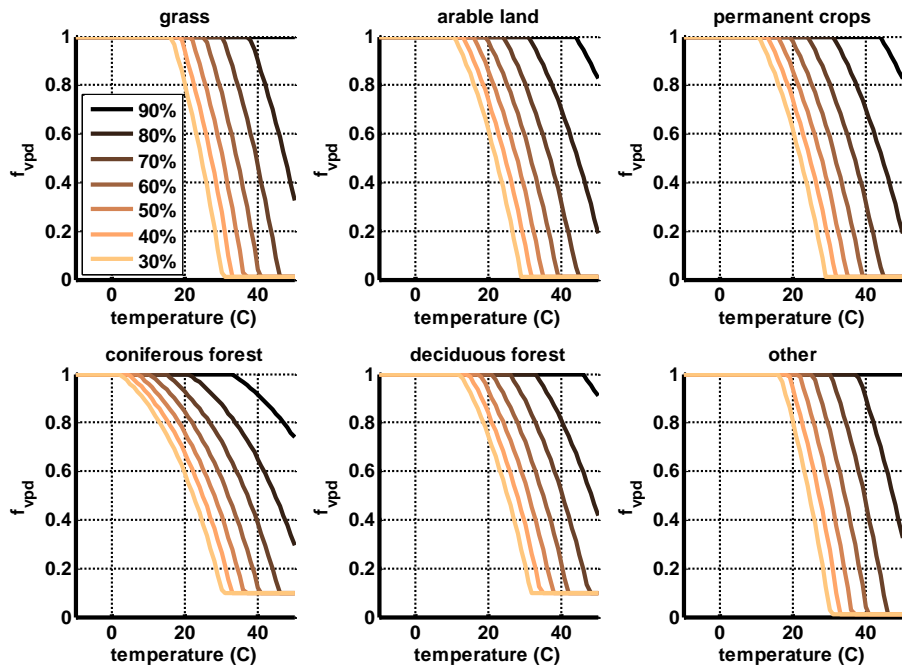


Figure 11. Correction factor for vapour pressure deficit  $f_{vdp}$  (Emberson), for relative humidity's of 30% - 90%. For normal conditions ( $T = 20\text{ }^{\circ}\text{C}$ ,  $\text{RH} > 70\%$ )  $f_{vdp} = 1$ , but for hot and dry conditions, large reductions are possible.

The correction factor for temperature is shown in Figure 12; its functional form is similar for all three parameterizations, but significant shifts of optimal temperature exist between the different parameterizations.

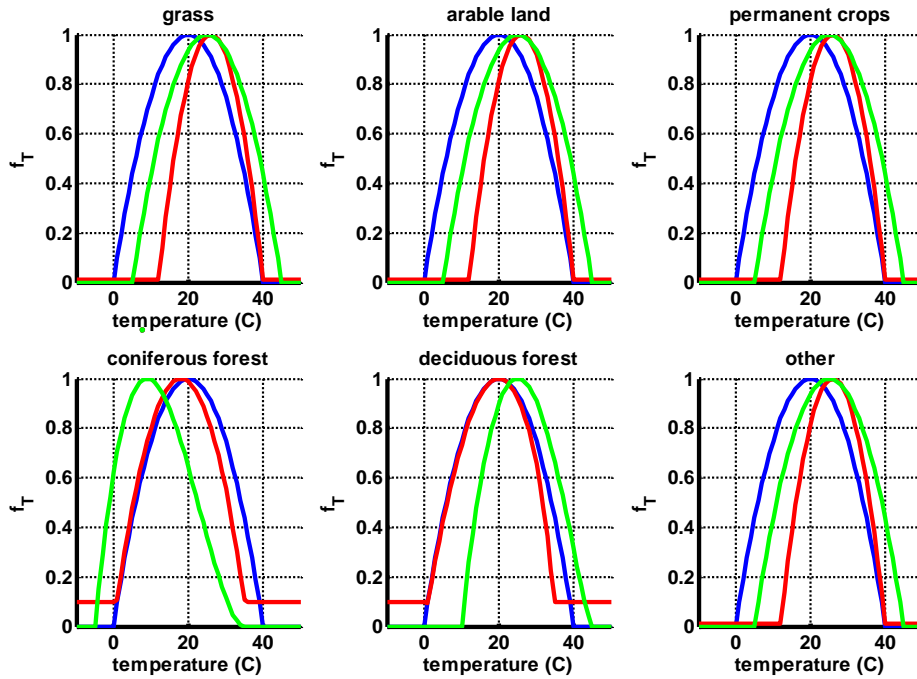


Figure 12. Correction factor for temperature; — Wesely, — Emberson, — Baldocchi.

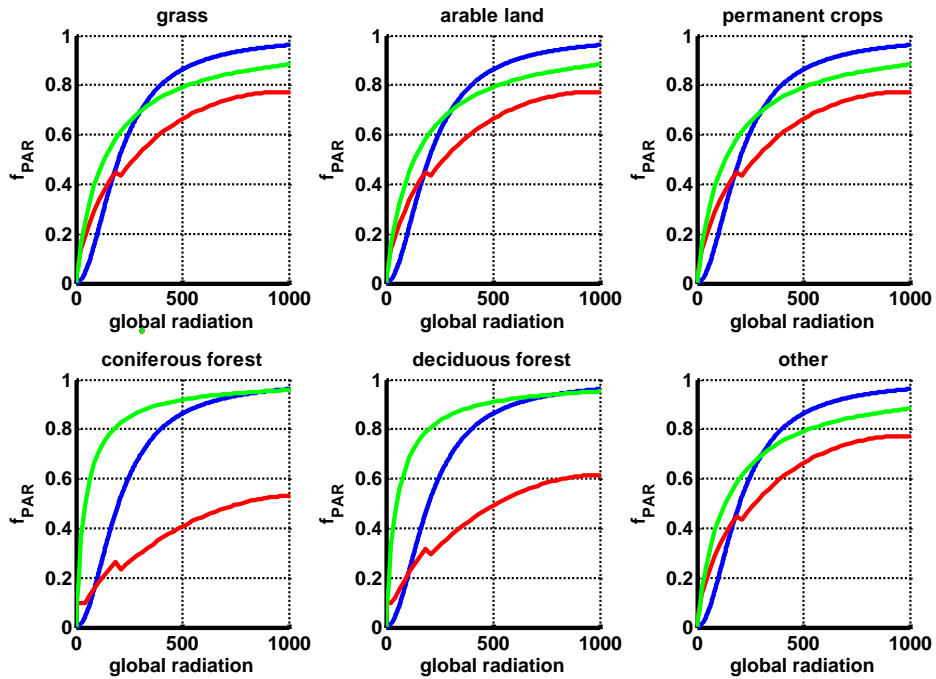


Figure 13. Correction factor for global radiation; cloud attenuation factor = 1 (clear sky)  
— Wesely, — Emberson, — Baldocchi.

In order to compute the correction factor for solar radiation, Emberson needs a model to compute the direct and diffuse parts of solar radiation. Following Zhang (2001), we used a parameterization by Weiss and Norman (1985), see Appendix C. In Appendix D., the effect of the radiation on sunlit and shaded leaves is parameterized, according to Norman (1982) and Zhang (2001). Wesely and DEPAC's implementation of Baldocchi use a radiation factor that does not take into account the difference between sunlit and shaded leaves.

The main difference between the different land use types is the value of the parameter  $\alpha$  in the exponential function  $f_{PAR} = 1 - \exp(-\alpha PAR)$  that is used for sunlit and shaded leaves. The parameter  $\alpha$  varies between 0.006 for *forest* and 0.009 ( $\mu\text{mol}/\text{m}^2/\text{s}$ )<sup>-1</sup> for *grass*, *arable land*, *permanent crops*, *other*.

The correction factor for phenology is only used by Emberson. It is shown that for the current land use types, the influence of this factor is not important and we will not use this factor (Appendix B).

The resulting stomatal conductances for different cloud attenuation factors of 1 (clear sky), 0.5 and 0.2 (overcast), are shown in the next three figures.

#### Conclusions for stomatal conductance

- Wesely's conductances are nearly always much lower than those of Baldocchi and Emberson. This is due to the much lower value of the maximal stomatal conductance.
- Differences between Emberson and our implementation of Baldocchi are mainly due to different parameterizations of the  $f_{par}$  correction factor.

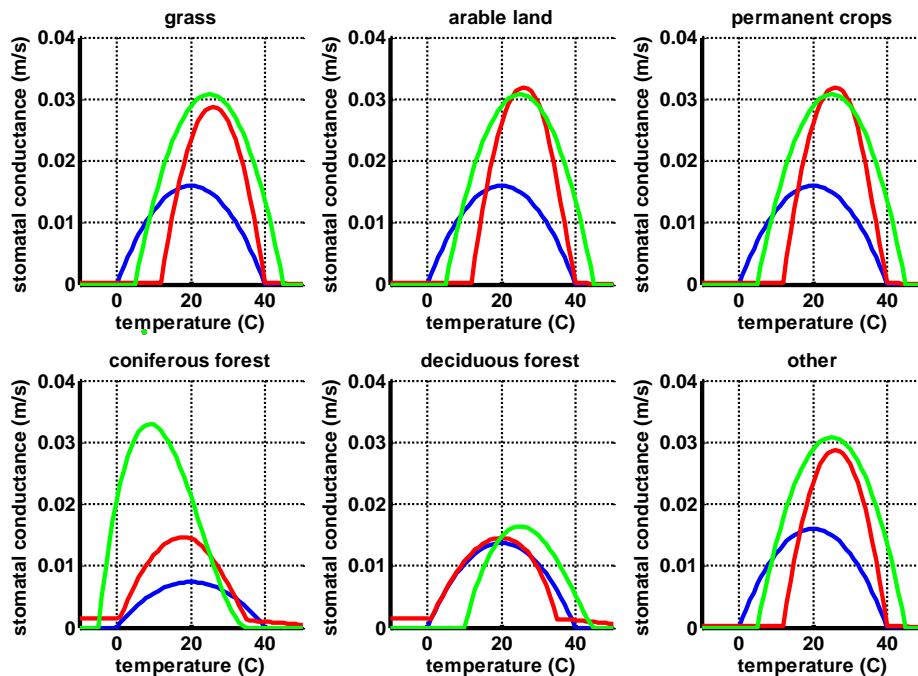


Figure 14. Stomatal conductance (m/s) for ammonia; cloud attenuation factor = 1 (clear sky), July, relative humidity = 80%, solar elevation = 50 degrees, global radiation = 958 W/m<sup>2</sup>.

— Wesely, — Emberson, — ≈Baldocchi.

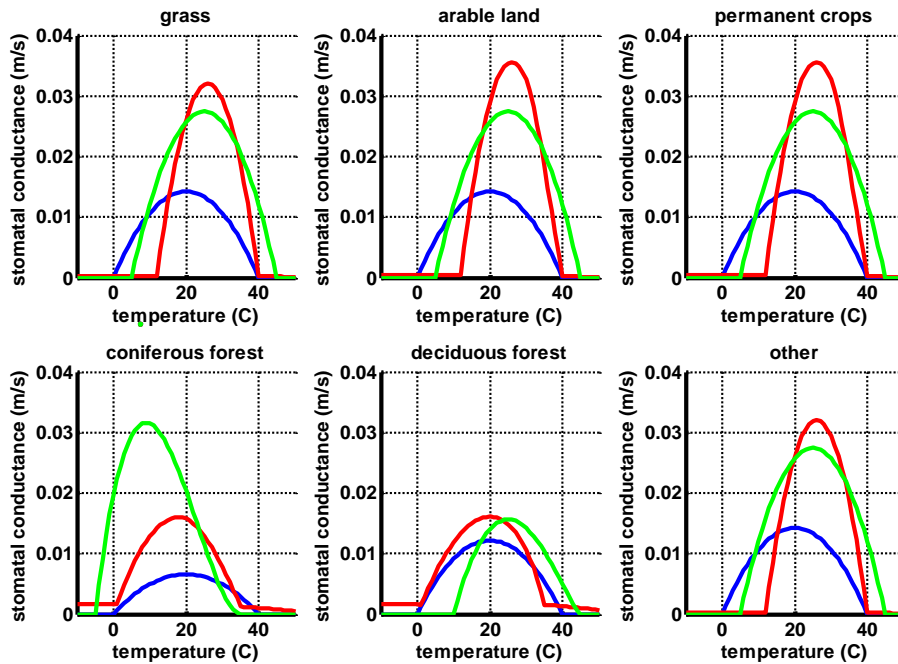


Figure 15. Stomatal conductance (m/s) for ammonia; cloud attenuation factor = 0.5, July, relative humidity = 80%, solar elevation = 50 degrees, global radiation = 479 W/m<sup>2</sup>.

— Wesely, — Emberson, — Baldocchi.

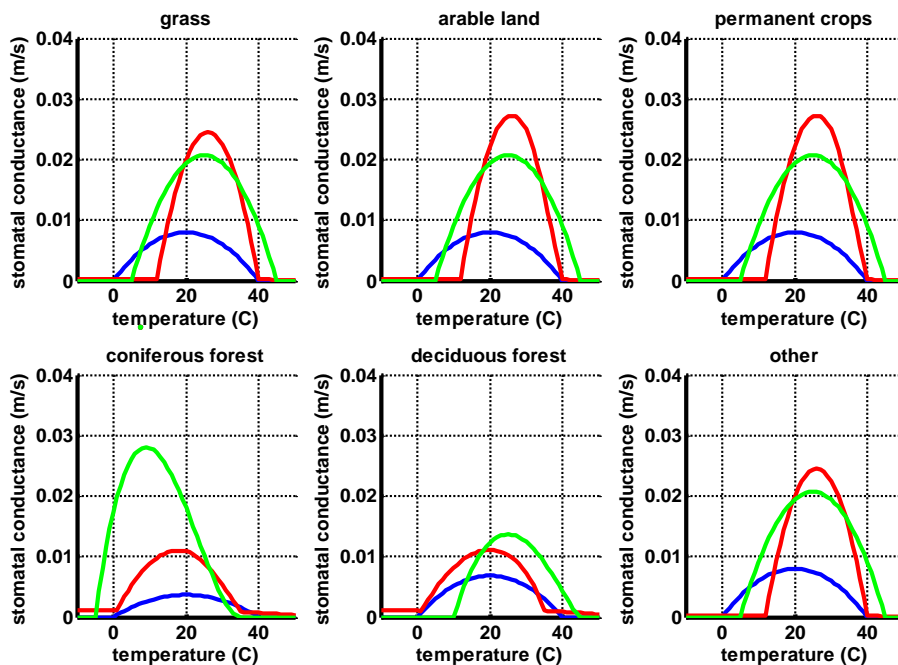


Figure 16. Stomatal conductance (m/s) for ammonia; cloud attenuation factor = 0.2 (overcast), global radiation = 192 W/m<sup>2</sup>, other specifications as Figure 15.





## Appendix F. Compensation points

This appendix shows parameterizations and graphs for the concentration in leaf stomata, at the external leaf surface or at the soil surface; these concentrations are, for historic reasons, called compensation points. Parameterizations are from Wichink Kruit et al. (2010).

### External leaf compensation point

$T_s$  is the leaf surface temperature (in °C),  $\chi_{a,4m}$  is the atmospheric ammonia concentration at 4 m height in  $\mu\text{g m}^{-3}$ ,  $\Gamma_w$  is the dimensionless molar ratio between the  $\text{NH}_4^+$  and  $\text{H}^+$  concentrations in the external leaf surface water:

$$\Gamma_w = 1.84 \cdot 10^3 \cdot \chi_{a,4m} \cdot \exp(-0.11 \cdot T_s) - 850. \quad \text{F.1.}$$

The functional behaviour of  $\Gamma_w$  as a function of temperature and atmospheric concentration is shown in Figure 17.

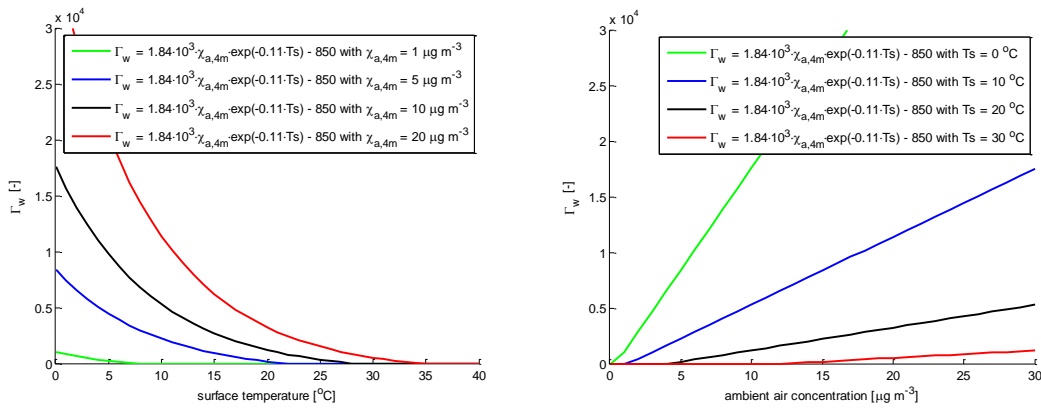


Figure 17.  $\Gamma_w$  as a function of the surface temperature for four different atmospheric ammonia concentrations (left panel);  $\Gamma_w$  as a function of the ambient air concentration for four different temperatures (right panel).

$\chi_w$  is the gaseous  $\text{NH}_3$  concentration at the external leaf surface (in  $\mu\text{g m}^{-3}$ ):

$$\chi_w = \frac{2.75 \cdot 10^{15}}{T_s + 273.15} \exp\left(\frac{-1.04 \cdot 10^4}{T_s + 273.15}\right) \cdot \Gamma_w. \quad \text{F.2.}$$

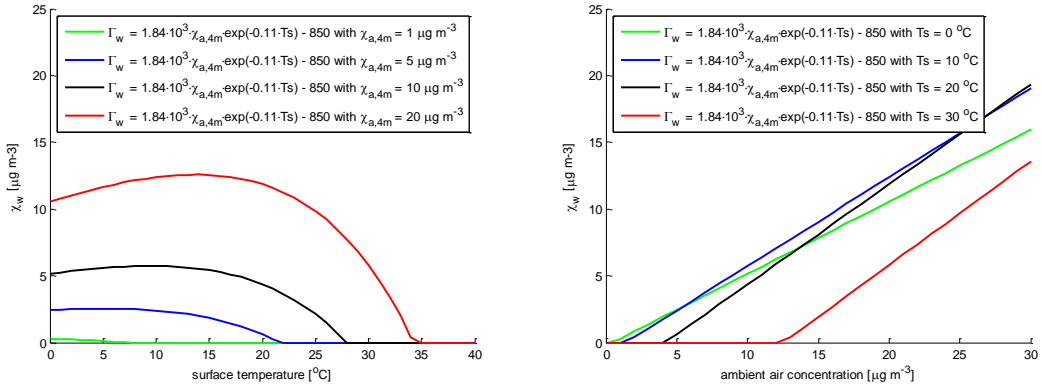


Figure 18.  $\chi_w$  as a function of the surface temperature for four different atmospheric ammonia concentrations (left panel);  $\chi_w$  as a function of the ambient air concentration for four different temperatures (right panel).

### Stomatal compensation point

$T_s$  is the leaf surface temperature (in °C) and  $\Gamma_s$  is the dimensionless ratio between the apoplastic molar  $\text{NH}_4^+$  and  $\text{H}^+$  concentration:

$$\Gamma_s(T_s) = \Gamma_{s, \text{micromet}} \cdot 4.7 \cdot \exp(-0.071 \cdot T_s), \quad \text{F.3.}$$

where  $\Gamma_{s, \text{micromet}} = 362 \cdot \chi_{a,4m}(\text{'long-term'})$  derived from micrometeorological measurements for the single-layer canopy compensation point model and  $\chi_{a,4m}(\text{'long-term'})$  is the 'long-term' atmospheric  $\text{NH}_3$  concentration at four meters height.

The functional behaviour of  $\Gamma_s$  is shown in Figure 19.

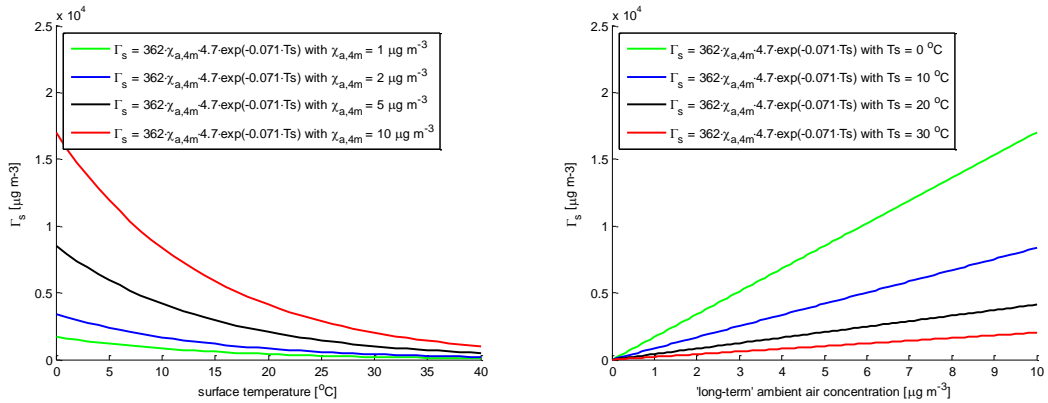


Figure 19.  $\Gamma_s$  as a function of the surface temperature for four different 'long-term' atmospheric ammonia concentrations (left panel);  $\Gamma_s$  as a function of the ambient air concentration for four different temperatures (right panel).

The stomatal compensation point  $\chi_s$  (in  $\mu\text{g m}^{-3}$ ) is:

$$\chi_s = \frac{2.75 \cdot 10^{15}}{T_s + 273.15} \exp\left(\frac{-1.04 \cdot 10^4}{T_s + 273.15}\right) \cdot \Gamma_s. \quad \text{F.4.}$$

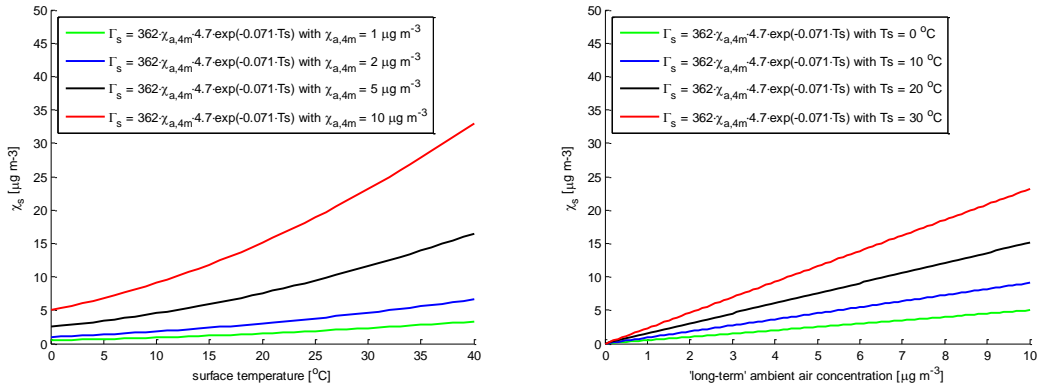


Figure 20.  $\chi_s$  as a function of the surface temperature for four different 'long-term' atmospheric ammonia concentrations (left panel) and  $\chi_s$  as a function of the ambient air concentration for four different temperatures (right panel).

### Water compensation point

Parameterizations are based on five years of data (2004–2008) from the Waterbase data of Rijkswaterstaat ([www.waterbase.nl](http://www.waterbase.nl)). Based on the 25 available measurement sites, the following yearly cycle of water temperature has been derived:

$$T_{water} = 13.05 + 8.3 \sin(DOY - 113.5) \text{ } ^{\circ}\text{C} \quad \text{F.5.}$$

with  $DOY$  = day of year.

This parameterization is based on best sinus fits for each individual site (25 in total). The spread in these fits is represented in the figure below by the bandwidth of the red lines. Next, a best fit of the median of all these fits was made, which is represented by the black dots in the figure. The red dots represent the median values of the individual fits.

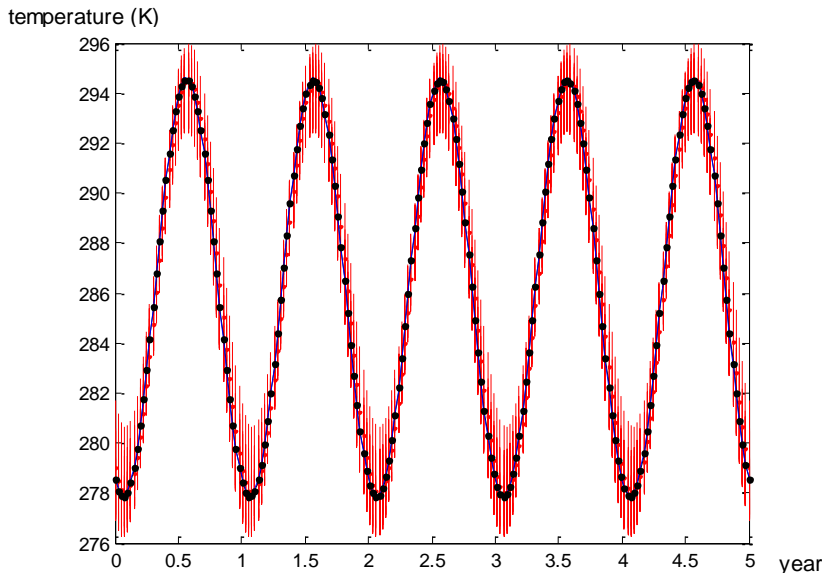


**Figure 21. Parameterization of the yearly cycle of water temperature (in [K]) projected for a period of five years. See text for detailed information.**

$\Gamma_{water}$  is the dimensionless molar ratio between the  $\text{NH}_4^+$  and  $\text{H}^+$  concentrations. From  $\text{NH}_4^+$  and pH measurements of 70 sites (of which the above mentioned 25 sites form a subset), a median value  $\Gamma_{water} = 430$  could be computed.

The temperature parameterization combined with  $\Gamma_{water}$  is used to calculate a parameterized  $\chi_{water}$  value:

$$\chi_{water} = \frac{2.75 \cdot 10^{15}}{T_{water} + 273.15} \exp\left(\frac{-1.04 \cdot 10^4}{T_{water} + 273.15}\right) \cdot \Gamma_{water} \quad \text{F.6.}$$

In the following figures the parameterized  $\chi_{water}$  values are compared with  $\text{NH}_3$  concentrations at several sites. The  $\text{NH}_3$  concentrations are derived from ammonia and pH measurements at these sites and represent the equilibrium concentrations just above the water surface.

The figures illustrate the representativeness of the F.6 parameterization (with a constant  $\Gamma_{water} = 430$ ) for the large fresh water bodies in The Netherlands (Figure 24) and the coastal waters (Figure 25). Further away at sea,  $\chi_{water}$  will be overestimated (lower panel Figure 25) while in polluted canals, rivers and lakes (Figure 22) the parameterization will underestimate  $\chi_{water}$ . However, using equation F.6. with a (more) site specific  $\Gamma_{water}$  will largely remove this under- or overestimation as is visible in the figures by the green dots. Simplifying equation F.6. even further by using one representative temperature value of 286.2 K (i.e. the yearly mean of equation F.5.) fixes the water compensation point at a value of roughly  $0.8 \mu\text{g m}^{-3}$ . This choice is visible in the figures with a red line.

Legend for all figures

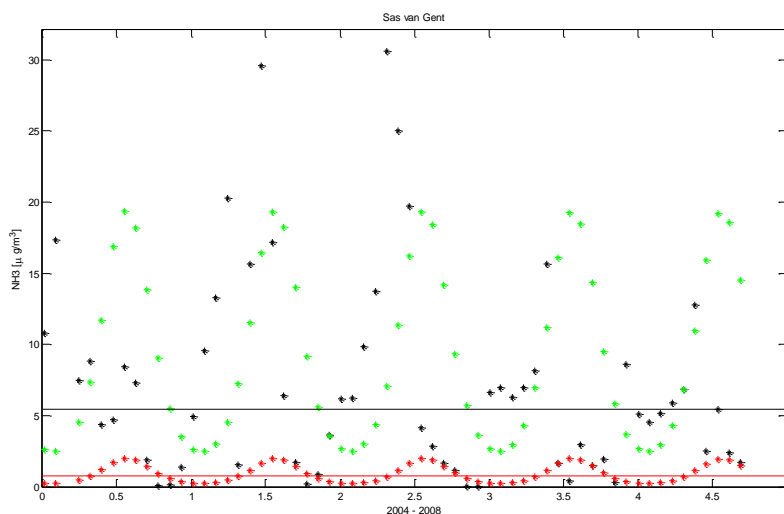
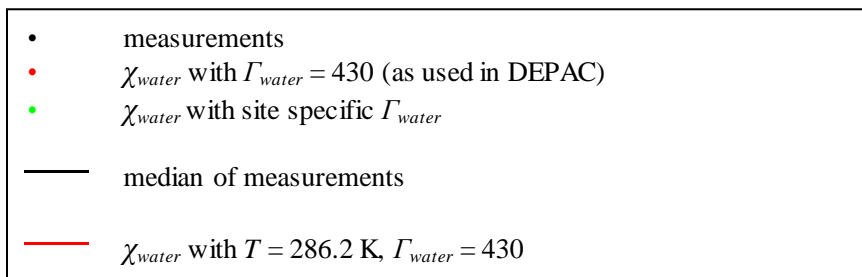


**Figure 22.** Values of measured and parameterized  $\text{NH}_3$  values at Sas van Gent. This site has the highest  $\text{NH}_3$  values in the Waterbase dataset and is an example of a site where the water compensation point parameterization underestimates the  $\chi_{water}$  value.

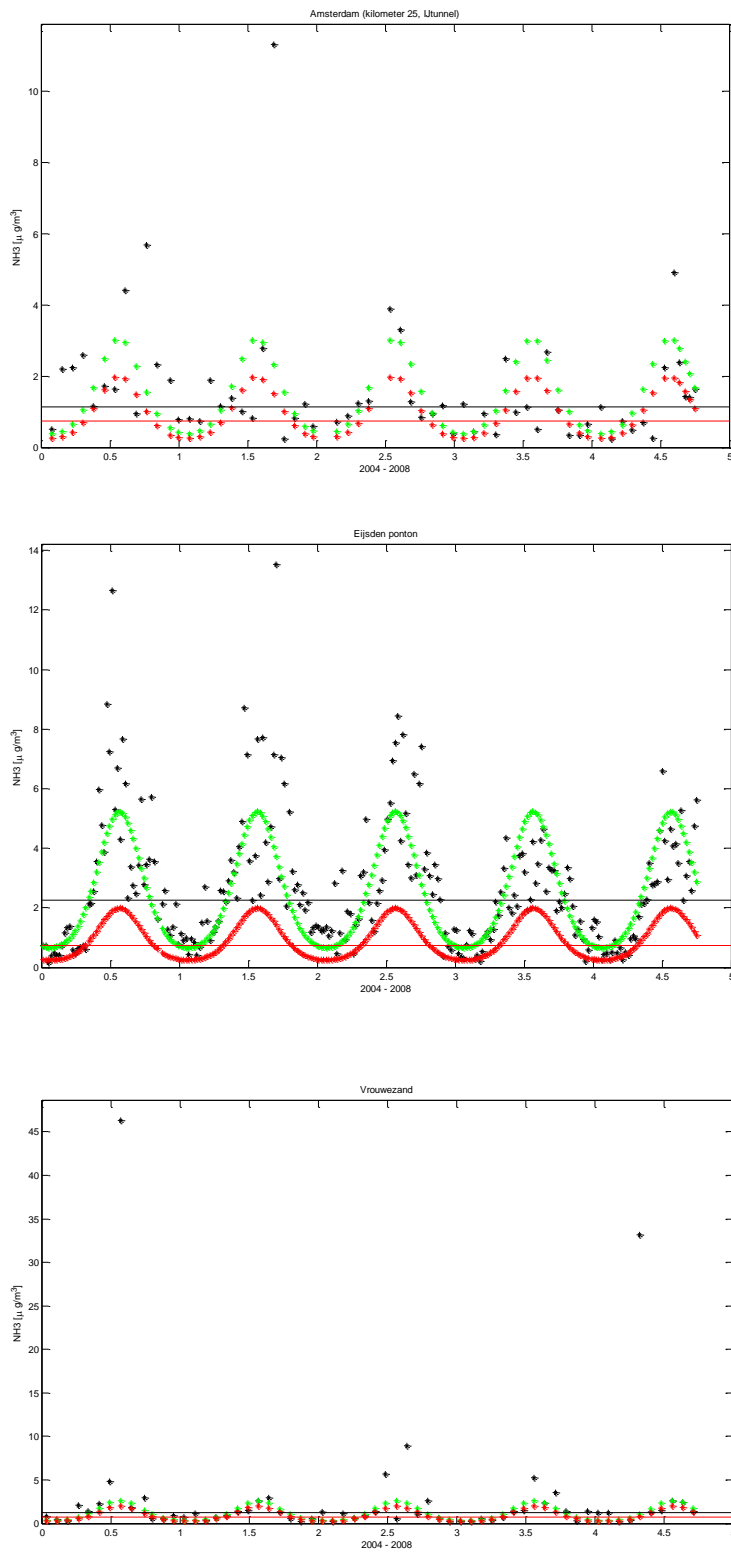


Figure 23. Examples of values of measured and parameterized  $\text{NH}_3$  values at river sites (Het IJ (Amsterdam), the Rhine (Lobith) and the Maas (Eijsden)). At these locations the parameterization is fairly representative.

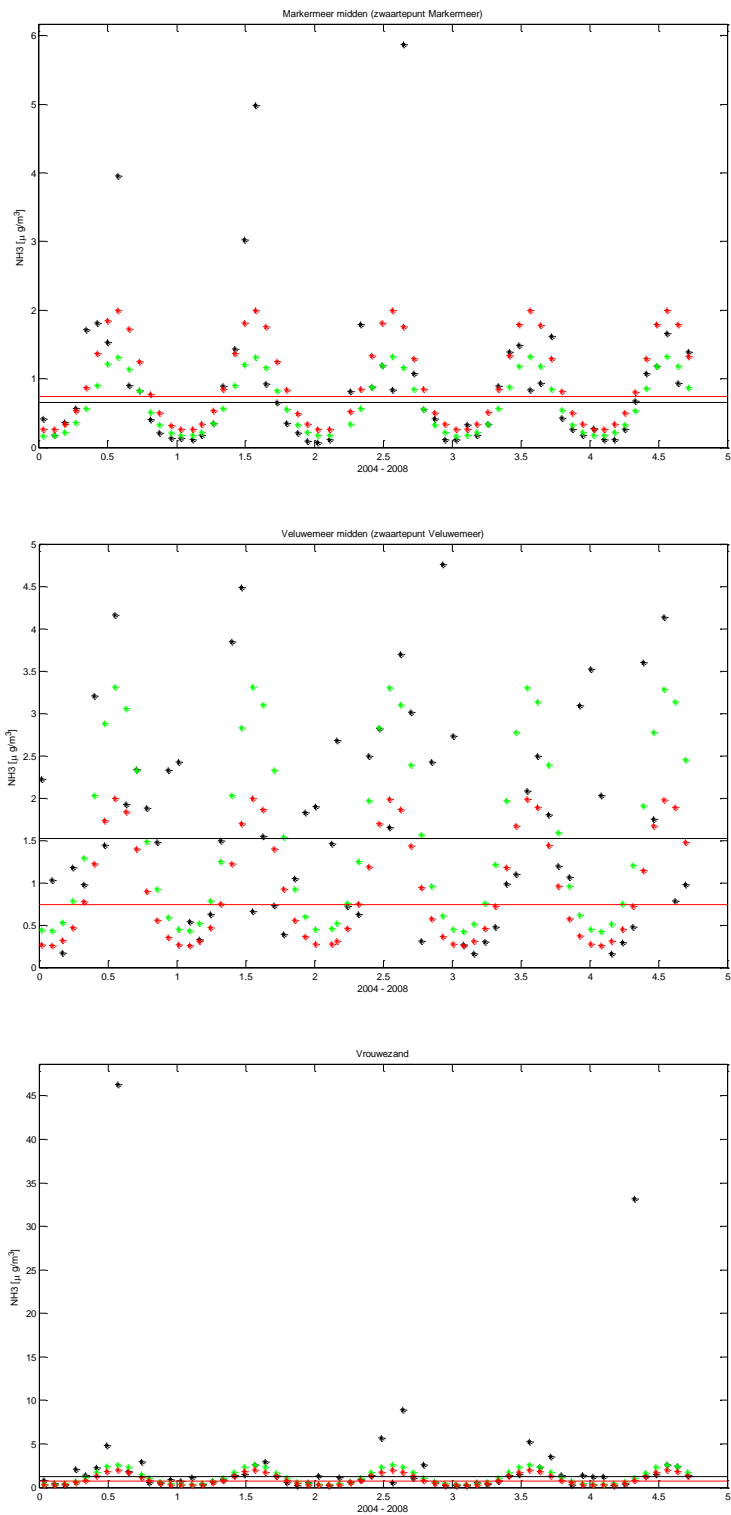
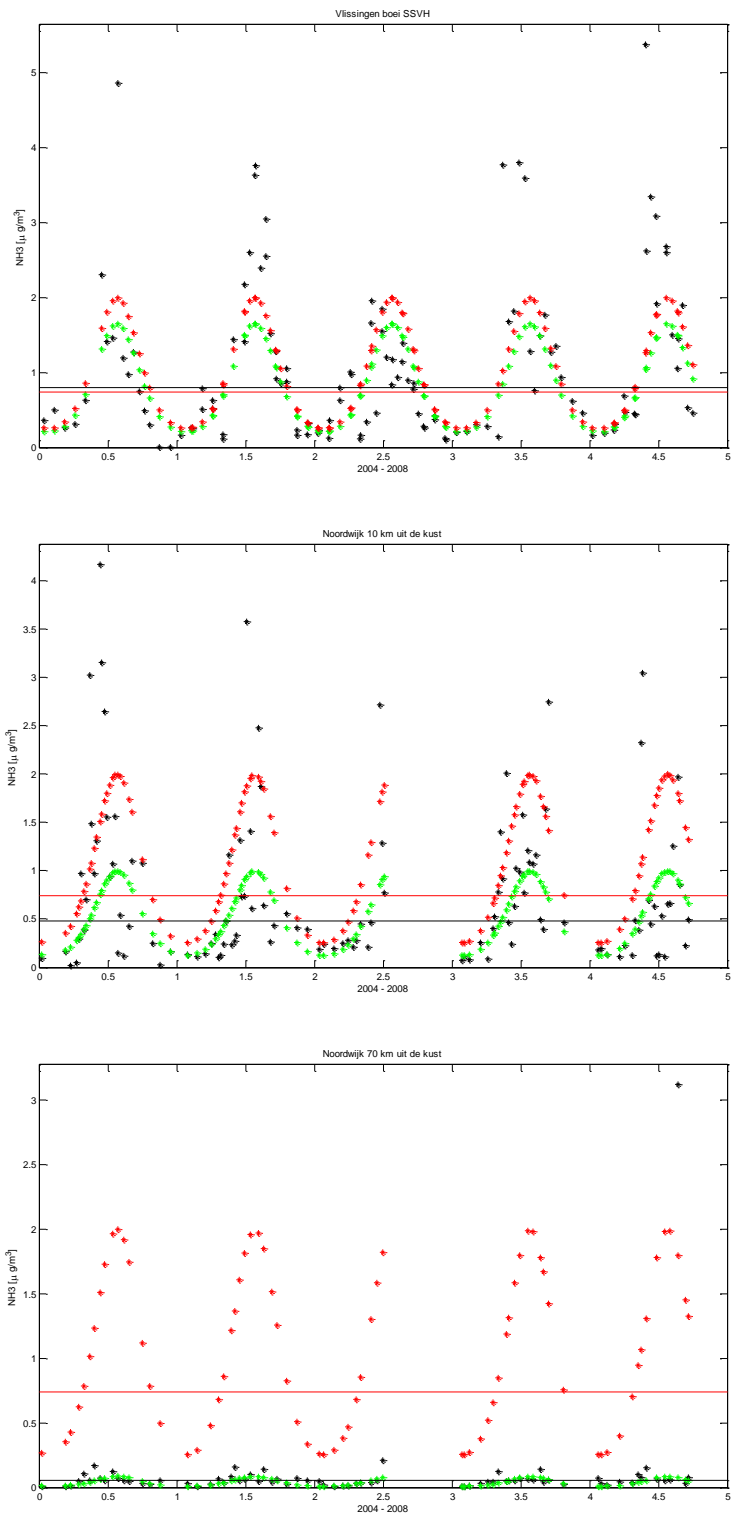


Figure 24. Examples of values of measured and parameterized  $\text{NH}_3$  values at the large fresh water bodies (IJsselmeer (Vrouwezand), Markermeer and Veluwemeer). At these locations the parameterization is representative.



**Figure 25. Values of measured and parameterized  $\text{NH}_3$  values at several salt water locations (Westerschelde (Vlissingen), North Sea (Noordwijk 10 and 70 km from the coast)). It is clearly visible that the closer to the coast, the more representative the parameterization is.**



## Appendix G. Fluxes and mass balance

The fluxes  $F$  over the different pathways in Figure 1 are:

$$F_1 = -\frac{(\chi_a - \chi_c)}{R_a + R_b}, F_2 = -\frac{(\chi_c - \chi_w)}{R_w}, F_3 = -\frac{(\chi_c - \chi_{soil})}{R_{soil,eff}}, F_4 = -\frac{(\chi_c - \chi_s)}{R_s}, \quad G.1.$$

with

- $\chi_a$  : atmospheric concentration ( $\mu\text{g}/\text{m}^3$ );
- $\chi_c$  : concentration at top of canopy ( $\mu\text{g}/\text{m}^3$ );
- $\chi_s$  : concentration in stomata ('stomatal compensation point') ( $\mu\text{g}/\text{m}^3$ );
- $\chi_w$  : external leaf compensation point ( $\mu\text{g}/\text{m}^3$ );
- $\chi_{soil}$  : soil compensation point ( $\mu\text{g}/\text{m}^3$ );
- $R_a$  : aerodynamic resistance (s/m);
- $R_b$  : quasi-laminar layer resistance (s/m);
- $R_w$  : external leaf (water layer) resistance (s/m);
- $R_{soil,eff}$  : effective soil resistance (s/m);
- $R_s$  : stomatal resistance (s/m).

Express the fluxes in terms of conductances  $G = \frac{1}{R}$  (and defining  $G_{ab} = \frac{1}{R_a + R_b}$ ):

$$F_1 = -G_{ab}(\chi_a - \chi_c), F_2 = -G_w(\chi_c - \chi_w), F_3 = -G_{soil,eff}(\chi_c - \chi_{soil}), F_4 = -G_s(\chi_c - \chi_s), \quad G.2.$$

Define the canopy conductance  $G_c = G_w + G_{soil,eff} + G_s$  and

$$\text{exchange velocity } V_e = \frac{1}{R_a + R_b + R_c},$$

we can now use the flux equation  $F_1 = F_2 + F_3 + F_4$  to eliminate  $\chi_c$ :

$$\begin{aligned} F_1 = F_2 + F_3 + F_4 &\Leftrightarrow G_{ab}(\chi_a - \chi_c) = G_w(\chi_c - \chi_w) + G_{soil,eff}(\chi_c - \chi_{soil}) + G_s(\chi_c - \chi_s) \Leftrightarrow \\ \chi_c(G_{ab} + G_w + G_{soil,eff} + G_s) &= G_{ab}\chi_a + G_w\chi_w + G_{soil,eff}\chi_{soil} + G_s\chi_s \Leftrightarrow \\ \chi_c(G_{ab} + G_c) &= G_{ab}\chi_a + G_c \left[ \frac{G_w}{G_c}\chi_w + \frac{G_{soil,eff}}{G_c}\chi_{soil} + \frac{G_s}{G_c}\chi_s \right]. \end{aligned} \quad G.3.$$

Defining the total compensation point as a weighed average of separate compensation points:

$$\chi_{tot} = \left[ \frac{G_w}{G_c}\chi_w + \frac{G_{soil,eff}}{G_c}\chi_{soil} + \frac{G_s}{G_c}\chi_s \right], \quad G.4.$$

we get

$$\chi_c = \frac{G_{ab}\chi_a + G_c\chi_{tot}}{(G_{ab} + G_c)}. \quad G.5.$$

Note that this equation is equivalent to equation (11) in Sutton (1998).

The flux  $F_1$  is:

$$\begin{aligned}
 F_1 &= -G_{ab}(\chi_a - \chi_c) = -G_{ab}\left(\chi_a - \frac{G_{ab}\chi_a + G_c\chi_{tot}}{G_{ab} + G_c}\right) = -G_{ab}\left(\frac{G_{ab}\chi_a + G_c\chi_a - G_{ab}\chi_a - G_c\chi_{tot}}{G_{ab} + G_c}\right) = \\
 &= -\left(\frac{G_{ab}G_c}{G_{ab} + G_c}\right)(\chi_a - \chi_{tot}) = -\left(\frac{1}{\frac{1}{G_{ab}} + \frac{1}{G_c}}\right)(\chi_a - \chi_{tot}) = -\left(\frac{1}{R_a + R_b + R_c}\right)(\chi_a - \chi_{tot}) = \\
 &= -V_e(\chi_a - \chi_{tot}).
 \end{aligned} \tag{G.6}$$

The mass balance in a layer with height  $H$  is:

$$H \frac{\partial \chi_a}{\partial t} = F_1 = -V_e \cdot (\chi_a - \chi_{tot}), \tag{G.7}$$

If we assume a constant value of  $\chi_{tot}$  (large reservoir), we get as solution

$$\chi_a(t) = \chi_{tot} + (\chi_a(0) - \chi_{tot}) \cdot \exp\left(-\frac{V_e}{H} \cdot t\right), \text{ starting from time } 0. \tag{G.8}$$

Alternatively, if we start from time  $t$  and perform a time step of  $\Delta t$ :

$$\chi_a(t + \Delta t) = \chi_{tot} + (\chi_a(t) - \chi_{tot}) \cdot \exp\left(-\frac{V_e}{H} \cdot \Delta t\right). \tag{G.9}$$

### Canopy compensation point model, effective resistance method

In this method (Asman, 1994), the same set-up of resistances is used as in the previous section, but we now want to compute a corrected exchange velocity  $V_e'$  and a corrected or 'effective' canopy resistance  $R_c'$ , such that we can still use the 'normal' formulas for deposition velocity and deposition flux:

$$F_1 = -V_e' \cdot \chi_a, \quad V_e' = \frac{1}{R_a + R_b + R_c'}. \tag{G.10}$$

This means that the term  $V_e \cdot \chi_{tot}$  from the previous section is moved into  $R_c'$ :

$$F_1 = -V_e \cdot (\chi_a - \chi_{tot}) = -V_e' \chi_a \tag{G.11}$$

from which follows

$$V_e' = V_e \left(\frac{\chi_a - \chi_{tot}}{\chi_a}\right) \tag{G.12}$$

and

$$\begin{aligned}
 R_c' &= \frac{1}{V_e'} - R_a - R_b = \frac{1}{V_e' \left( \frac{\chi_a - \chi_{tot}}{\chi_a} \right)} - R_a - R_b = \frac{R_a + R_b + R_c}{\left( \frac{\chi_a - \chi_{tot}}{\chi_a} \right)} - R_a - R_b \\
 &= \left( \frac{\chi_a}{\chi_a - \chi_{tot}} \right) (R_a + R_b + R_c) - \frac{(\chi_a - \chi_{tot})(R_a + R_b)}{(\chi_a - \chi_{tot})} = \left( \frac{(R_a + R_b)\chi_{tot} + R_c\chi_a}{(\chi_a - \chi_{tot})} \right). \quad \text{G.13.}
 \end{aligned}$$

Note that the effective resistance is negative in the case of an emission flux ( $\chi_a < \chi_{tot}$ ).

The mass balance in a layer with height  $H$  can now be solved as follows:

$$H \frac{\partial \chi_a}{\partial t} = F = -V_e' \cdot \chi_a \quad \text{G.14.}$$

$$\chi_a(t + \Delta t) = \chi_a(t) \cdot \exp\left(-\frac{V_e'}{H} \cdot \Delta t\right). \quad \text{G.15.}$$

Note however that there are two flaws in this method:

- $\chi_a \rightarrow 0$ . In this case the corrected exchange velocity  $V_e'$  goes to infinity.
- In the differential equation for the mass balance, the coefficient  $V_e'$  is treated as a constant, but it depends on the independent variable  $\chi_a$ .



## Appendix H. Implementation issues

This appendix contains a list of (corrected) bugs and remarks on the implementation of DEPAC into OPS and LOTOS-EUROS. It also presents former differences between the OPS and LOTOS-EUROS implementations of DEPAC. In DEPAC v.3.11 these differences are straightened. Note that the bugs in the Emberson and Baldocchi parameterizations of stomatal resistance did not appear in previous operational versions of OPS and/or LOTOS-EUROS, since there the Wesely parameterization has been used.

### DEPAC versions

Different versions of DEPAC existed, e.g. in the OPS and LOTOS-EUROS models. Part of the project of setting up a new DEPAC was to make a new module structure, that could be easily used by different models. Starting versions for this process were DEPAC/OPS-LT-v.4.1.17 and DEPAC/LE-v.1.3. Note that the parameterization of *R<sub>ext</sub>* in v3.7 is different than in v3.6: in v3.6, deposition via the external leaf surface is diminished by a higher *R<sub>ext</sub>* value (compared to older DEPAC versions), in v3.7, this is accomplished by an external compensation point.

version	used in model	
OPS-LT	OPS long term model, version 4.1.17	
OPS-KT	OPS short term model, version 3.0.2	
LE	LOTOS-EUROS, version 1.3	
version	based on version	new with respect to 'based on' version
v2		compensation point (ref. Sutton 1998 AE 473-480) new parameterization of <i>R<sub>w</sub></i> (Sutton). Warning: the component numbering is different as in other DEPAC versions ( <i>O<sub>3</sub></i> is added as component 1). V2 has been used for experimental versions of OPS.
3.0	OPS-LT/ OPS-KT/LE	synthesis of different DEPAC versions; new module structure: separate routines are called for each component.
3.1	3.0	test version, not used anymore.
3.2	3.0	new module structure, where separate routines are called for different deposition paths (e.g. soil, external leaf, stomata). The components are dealt with inside these routines.
3.3	3.2	bug fixed in the computation of the leaf area index.
3.3.1	3.3	leaf area index included in <i>R<sub>w</sub></i> .
3.4	3.3	<i>R<sub>soil</sub></i> (NH <sub>3</sub> ,urban) = 100 s/m (was 1000 s/m).
3.4.1	3.4	leaf area index included in <i>R<sub>w</sub></i> .
3.5	3.4	<i>R<sub>inc</sub></i> (grass) = ∞ (was 0 s/m).
3.5.1	3.5	leaf area index included in <i>R<sub>w</sub></i> .
3.6	3.5	new parameterization of <i>R<sub>w</sub></i> (Wichink Kruit, Aug. 2008) stomatal compensation point for NH <sub>3</sub> .

3.6.1	3.6	leaf area index included in $R_w$ .
3.7	3.6	new parameterization of $R_w$ (Wichink Kruit, Mar. 2009) stomatal and external leaf compensation points for $\text{NH}_3$ Wesely's parameterization for stomatal resistance.
3.7.1	3.7	leaf area index included in $R_w$ .
3.8	3.7	Baldocchi's parameterization for stomatal resistance.
3.8.1	3.8	leaf area index included in $R_w$ .
3.8.2	3.8.1	bug fix for optimal temperature in Baldocchi.
3.9	3.8.1	Emberson's parameterization for stomatal resistance. PAR computations for shaded, sunlit leaves update $\Gamma$ -parameterization according to Wichink Kruit (2010).
3.10	3.9	new LAI, SAI soil compensation point for water.
3.11	3.10	all obsolete code removed. differences LOTOS-EUROS and OPS straightened.
depac_GC2010	3.11 and 3.3	shell around DEPAC 3.11 (for $\text{NH}_3$ ) and DEPAC 3.3 (other components).

### General implementation issues

#### *Leaf area index in external leaf resistance*

In DEPAC versions /OPS, /LE, v3.0 – v3.8, the leaf area index was not included in the computation of the external leaf resistance  $R_w$ . Since the  $R_w$  parameterization is derived from data at grassland at the Haarweg measuring site, the corresponding conductance ( $G_w$ ) for another land use type  $i$  has to be scaled as follows:

$$G_w(i) = \frac{SAI(i)}{SAI(Haarweg)} G_w(i).$$

In the case of freezing temperatures  $r_w$  is fixed at 200 s/m and the canopy conductance is  $G_w = SAI / r_w$ .

#### *Stomatal resistance (Wesely)*

In routine *stowes*, the stomatal resistance is computed according to Wesely;  $t$ : temperature ( $^{\circ}\text{C}$ ),  $glrad$ : global radiation,  $ri$ : minimal stomatal resistance;  $rs$ : stomatal resistance,  $gs$ : stomatal conductance (output).

```

if (t.ne.0) then
  rs = ri*(1 + (200/(glrad + 0.1))**2)*(400/(t*(40-t)))
else
  rs = ri
endif
if (rs.gt.0) then    !i.e. check on 0 < t > 40C
  gs = 1/rs
else
  gs = 0
endif

```

A bug appears if  $Ri = -999$  and  $T < 0$  °C (or  $T > 40$  °C), then  $R_s$  is positive again and  $g_s = 1/R_s$ . In most of these cases  $g_s$  will be very small ( $g_{lrad} = 0$  W/m<sup>2</sup>,  $T = -20$  °C  $\rightarrow g_s = 8 \cdot 10^{-10}$  m/s; extreme value at  $g_{lrad} = 1000$  W/m<sup>2</sup>,  $T = -20$  °C  $\rightarrow g_s = 3 \cdot 10^{-3}$  m/s). Bug fix: extra check for  $Ri > 0$ .

If  $T = 0$ , then  $R_s = Ri$  and  $g_s = 1/Ri$ ; this is not continuous with respect to temperature: if  $T \rightarrow 0$ , then  $R_s \rightarrow \infty$  and  $g_s \rightarrow 0$ . Bug fix: if  $T = 0 \rightarrow g_s = 0$ .

There is no check for  $T = 40$  °C.

The new code is:

```
if (ri > 0 .and. (0.0 .lt. t .and. t .lt. 40.0)) then
    rs = ri*(1 + (200/(glrad + 0.1))**2)*(400/(t*(40-t)))
    gs = 1/rs
else
    gs = 0.0
endif
```

This bug appears in OPS and LOTOS-EUROS versions of DEPAC. It has been fixed in all DEPAC versions since v.3.0.

#### Optimal temperature in Baldocchi

In routine *stobal* (OPS and LOTOS-EUROS versions) a parameter BT is defined in the temperature correction factor for stomatal conductance:

$$BT = (TH-TO) / (TH-TL),$$

$$GT = ((T-TL) / (TO-TL)) * ((TH-T) / (TH-TO)) ** BT$$

With:

- TL: lower temperature for stomata closure;
- TO: optimal temperature;
- TH: higher temperature for stomata closure;
- GT: temperature correction factor.

Formulas are from Jarvis, 1976. Using this expression for BT, the optimum temperature correction factor GT is reached at a temperature that does not coincide with the optimal temperature TO. Using the formula

$$BT = (TH-TO)/(TO-TL),$$

the optimum does occur at TO (see Figure 26).

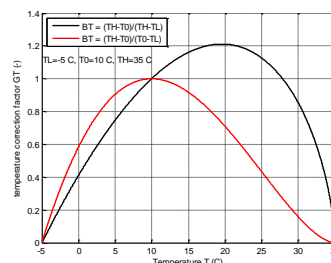
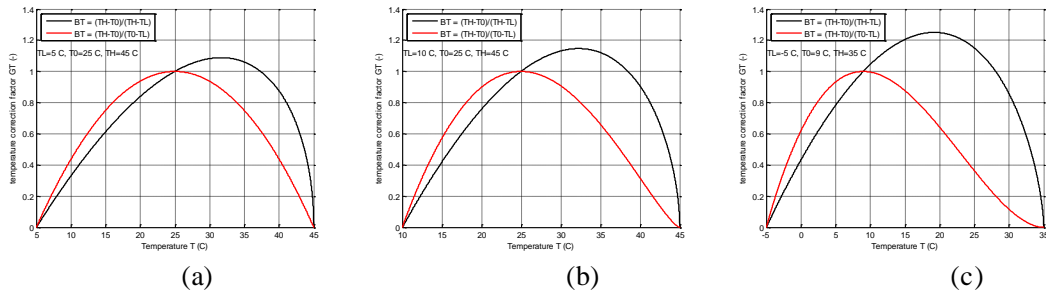


Figure 26. Temperature correction factor for two different expressions of parameter BT; the values of TL = -5 °C, TO = 10 °C, TH=35 °C are from the original paper of Jarvis, 1976.

The graph that reproduces the graph in Jarvis, 1976, is the red one, i.e. using  $BT = (TH-TO)/(TO-TL)$ .

On page 94, Baldocchi et al. (1987) presents a formula equivalent to that of Jarvis, which contains the same error. However, on page 97 of the same article it says: ‘The functional form presented by Jarvis (1976) for  $bt$  appears to be in error; a better form is  $bt = (T_{max} - T_o)/(T_o - T_{min})$ ’. Note: Emberson (2000a,b) uses the correct formula.

In the current DEPAC versions, three different sets of  $[TL, TO, TH]$  are used (Baldocchi et al., 1987):



**Figure 27. Temperature correction factor for two different expressions of parameter  $BT$  and different sets of  $[TL, TO, TH]$ :  $[5, 25, 45]$  °C for grass, arable land, permanent crops and other (a);  $[10, 25, 45]$  °C for deciduous forest (b);  $[-5, 9, 35]$  °C for coniferous forest (c).**

Note that, if you look at a 'moderate' daytime temperature range of 15-30 °C, differences between the two graphs are not so large; only for coniferous forest there are larger differences already at 20 °C.

## Implementation issues related to OPS

### Soil resistance, urban

The following statement, which is found in the OPS-versions of DEPAC, is meant to use the soil resistance  $r_{so}$  of water (Olsen land use class number 14), in the case of a wet, urban surface (Olson number 15, LBG number 7):

```
if (nwet.eq.1.and.lbg1u.eq.7) rso(15,icmp)=rso(14,icmp)
```

The statement is redundant: if  $nwet = 1$ ,  $rswet$  is used. Even worse, it gives cause to error, since  $r_{so}$  is not reset to its original value. As a consequence, if (inside a time loop in OPS) it gets wet ( $nwet = 1$ ), then  $r_{so}(\text{urban})$  will remain equal to  $r_{so}(\text{water})$ , even if it gets dry afterwards. In practice, this means that the soil resistance for  $NH_3$  in dry circumstances is that of a wet surface (10 s/m). This error is compiler dependent (depends on whether the compiler keeps  $r_{so}$  in memory).

### Stomatal resistance (Baldocchi) in OPS-KT

In routine *stobal* (computation of stomatal resistance according to Baldocchi), DEPAC crashes (divide by zero). This bug appears because the check on whether there is vegetation present in the current land use type (and whether to call *stobal*), is incorrect:

```
if (rsmin(lu).ne.-998) then
```



This has been replaced by

```
if (abs(rsmin(lu) + 999.) .GT. 1.0e-4) then
```

This bug only appears in DEPAC/OPS-KT.

### Implementation issues related to LOTOS-EUROS

#### Land use

The land use database used by LOTOS-EUROS starts from the official Corine/Phare Land Cover Data from the EEA (EEA, 2000), which was completed for the full European domain by Smiatek (FI-Garmisch Partenkirchen) using (mainly) the Pelinda database (De Boer et al., 2000). DEPAC uses nine land use classes

Smiatek	DEPAC
1. urban areas	1. grass
2. agriculture	2. arable land
3. grassland	3. permanent crops
4. deciduous forest	4. coniferous forest
5. coniferous forest	5. deciduous forest
6. mixed forest	6. water
7. water	7. urban
8. marsh or wetland	8. other, i.e. short grassy area
9. sand, bare rocks	9. desert
10. tundra	
11. permanent ice	
12. tropical forest	
13. woodland scrub	

The following conversion is used to ‘translate’ the Smiatek classification (in terms of fractions per grid cell) to the one used in DEPAC:

DEPAC	in terms of Smiatek land use indices	in terms of Smiatek land use classification
1 grass	3	grassland
2 arable land	$\frac{1}{2} * 2$	$\frac{1}{2}$ agriculture
3 permanent crops	$\frac{1}{2} * 2$	$\frac{1}{2}$ agriculture
4 coniferous forest	$5 + \frac{1}{2} * 6$	coniferous forest + $\frac{1}{2}$ mixed forest
5 deciduous forest	$4 + \frac{1}{2} * 6 + 12 + \frac{1}{2} * 8 + 13$	deciduous forest + $\frac{1}{2}$ mixed forest + tropical forest + $\frac{1}{2}$ (marsh or wetland) + woodland scrub
6 water	$7 + 11 + \frac{1}{2} * 8$	water + permanent ice + $\frac{1}{2}$ (marsh or wetland)
7 urban	1	urban areas
8 other	10	tundra
9 desert	9	sand, bare rocks

#### Seasonal factor leaf area index

Versions DEPAC/LE and DEPAC v.3.0, 3.1 and 3.2 have a bug in the seasonal factor for the leaf area index (slai). In the old slai-function, the wrong type of land use numbering is used. This bug (which was fixed in DEPAC v.3.3) has effect on land use types *permanent crops*, *coniferous forest* and *deciduous forest* and *other*. The OPS versions do not suffer from this bug.

#### *Stomatal resistance according to Emberson*

The original Emberson implementation in LOTOS-EUROS does not contain the correct dimensions for  $\alpha$  in the correction factor for radiation. In LOTOS-EUROS we have PAR in  $\text{W/m}^2$ , the dimension of  $\alpha$  is  $(\text{W/m}^2)^{-1}$ ; Emberson uses PAR in  $\mu\text{mol/m}^2/\text{s}$ . Therefore  $\alpha$  has to be scaled:  
 $\alpha (\text{W/m}^2)^{-1} = 4.57 \alpha (\mu\text{mol/m}^2/\text{s})^{-1}$ .

Emberson computes stomatal conductances for ozone; for other gases this has to be scaled with  $D(\text{gas})/D(\text{O}_3)$ , with  $D$ : diffusion coefficient ( $\text{m}^2/\text{s}$ ).

#### *Minimal value for stomatal resistance in Baldocchi*

$R_{s,\text{min}}$  for land use type *other* = -100 s/m, this should be 100 s/m.

#### *Default value for temperature factor in Baldocchi*

In the LOTOS-EUROS version of DEPAC, routine *stobal*, there is a bug in the temperature correction factor:

```
BT = (TH(lu)-T0(lu)) / (TH(lu)-TE(lu))
if (T.gt.TE(lu).and.T.lt.TH(lu)) then
    GT = ((T-TE(lu)) / (T0(lu)-TE(lu))) * ((TH(lu)-T) / (TH(lu)-T0(lu)))**BT
else
    GT = 1
endif
```

The default value (in the 'else' statement) should be 'GT = 0'.

### **Differences in DEPAC between LOTOS-EUROS and OPS**

There existed seven differences between the DEPAC code as in use in LOTOS-EUROS and in OPS, three for NO and four for SO<sub>2</sub>. All seven are discussed below and the option chosen in the current DEPAC version (v.3.11) is given with a justification. In DEPAC v.3.3 a switch exists to choose either the OPS or LOTOS-EUROS way, the default option is OPS.

#### *NO*

```
if (ipar_model == 1) then ! 1: OPS, 2: LOTOS-EUROS
    rsoil = (/ -999, -999, -999, -999, -999, 2000, 1000, -999, -999 /)
else
    rsoil = (/ -999, -999, -999, -999, -999, 2000, 1000, -999, 2000 /)
endif
```

LOTOS-EUROS option of resistance for desert of 2000 s/m is chosen, see Table 5 in Erisman et al 1994.

```
if (ipar_model == 1) then ! 1: OPS, 2: LOTOS-EUROS
    call rw_constant(10000.,gw)
```

```

else
  call rw_constant(2000.,gw)
endif

```

Neither the LOTOS-EUROS nor the OPS option is chosen, but the value is set to -9999 (Erisman et al., 1994).

```

if (ipar_model == 1) then
  ! OPS
  if (nwet .eq. 1 .and. lu .ne. 6 .and. lu .ne. 7) then
    ! (wet) ^ (not water) ^ (not urban)
    if (missing(rsoil_wet)) then
      rc_tot = -9999.
    else
      rc_tot = rsoil_wet
    endif
    ready = .true.
  else
    ! snow surface:
    if (nwet.eq.9) then
      call rc_snow(ipar_snow,t,rc_tot)
      ready = .true.
    endif
  endif
else
  ! LOTOS-EUROS
  if (lu .eq. 6) then ! water
    rc_tot = 2000.
    ready = .true.
  elseif (nwet .eq. 1) then ! wet
    rc_tot = 2000.
    ready = .true.
  elseif (nwet .eq. 9) then ! snow
    call rc_snow(ipar_snow,t,rc_tot)
    ready = .true.
  endif
endif
endif

```

LOTOS-EUROS option is chosen (rc\_tot = 2000 s/m for nwet = 1 and lu = 6).

### SO<sub>2</sub>

```

if (ipar_model == 1) then ! 1: OPS, 2: LOTOS-EUROS
  rsoil_wet = 10
else
  rsoil_wet = 50
endif

```

```

if (ipar_model == 1) then ! 1: OPS, 2: LOTOS-EUROS

```

```

    rsoil = (/ 1000, 1000, 1000, 1000, 1000, 10, 1000, 1000, 1000/)
else
    rsoil = (/ 1000, 1000, 1000, 1000, 1000, 50, 1000, 1000, 1000/)
endif

!-----
! wet surface
!-----
if (ipar_model == 1) then ! 1: OPS, 2: LOTOS-EUROS
    rw = 10.
else
    rw = 50.
endif

```

OPS option of resistance = 10 s/m in 'wet' cases is chosen, see Table 5 in Erisman et al 1994 (here 0 is interpreted as 'negligible' and the corresponding resistance is set to 10 s/m).

```

!-----
! dry surface
!-----
if (ipar_model == 1) then ! 1: OPS, 2: LOTOS-EUROS
    ! T > -1 C
    if (t .gt. -1.0) then
        if (rh .lt. 81.3) then
            rw = 25000*exp(-0.0693*rh)
        else
            rw = 0.58e12*exp(-0.278*rh) + 10.
        endif
    else
        ! -5 C < T <= -1 C
        if (t .gt. -5.0) then
            rw=200
        else
            ! T <= -5 C
            rw=500
        endif
    endif
else
    if (rh .lt. 81.3) then
        rw = 25000.*exp(-0.0693*rh)
    else
        rw = 0.58e12*exp(-0.278*rh) + 50.
    endif
endif
endif

```

OPS option is chosen, since this is according to DEPAC documentation in Erisman et al 1994, page 2598.